NASA TECHNICAL NOTE

NASA TN D-6056

NASA TN D-6056

c. 1

METEOROID HAZARD EVALUATION FOR SIMPLE STRUCTURES WITH VARIOUS ORIENTATIONS

by C. D. Miller

Lewis Research Center
Cleveland, Ohio 44135

NATIONAL AERONAUTICS AND SPACE ADMINISTRATION • WASHINGTON, D. C. • OCTOBER 1970

1. Report No.	2. Government Accession No.	3. Recip... Catalog No.
NASA TN D-6056		

4. Title and Subtitle
METEOROID HAZARD EVALUATION FOR SIMPLE STRUCTURES WITH VARIOUS ORIENTATIONS

5. Report Date
October 1970

6. Performing Organization Code

7. Author(s)
C. D. Miller

8. Performing Organization Report No.
E-5107

9. Performing Organization Name and Address
Lewis Research Center
National Aeronautics and Space Administration
Cleveland, Ohio 44135

10. Work Unit No.
131-05

11. Contract or Grant No.

12. Sponsoring Agency Name and Address
National Aeronautics and Space Administration
Washington, D.C. 20546

13. Type of Report and Period Covered
Technical Note

14. Sponsoring Agency Code

15. Supplementary Notes

16. Abstract

A statistical analysis was performed with use of Smithsonian Astrophysical Observatory's data on photographic meteors with use of weighting factors developed at Lewis Research Center for correction of various biases involved in meteor photography. The analysis used an armor damage criterion supplied by Ames Research Center. Although the analysis was restricted to Earth's orbit about Sun, implications are discussed regarding total population of meteoroids throughout the solar system. In Earth's orbit about the Sun, advantage was found for cylindrical armor extending in the solar direction and a plane sheet alined normal to apex of Earth movement.

17. Key Words (Suggested by Author(s))
Meteor
Meteoroid
Hazard
Analysis
Statistical
Space
Armor

18. Distribution Statement
Unclassified - unlimited

19. Security Classif. (of this report)	20. Security Classif. (of this page)	21. No. of Pages	22. Price*
Unclassified	Unclassified	70	$3.00

*For sale by the Clearinghouse for Federal Scientific and Technical Information
Springfield, Virginia 22151

CONTENTS

METEOROID HAZARD EVALUATION FOR SIMPLE STRUCTURES WITH VARIOUS ORIENTATIONS

by C. D. Miller

Lewis Research Center

SUMMARY

An analysis was performed on the effects of orientation of planes and cylinders upon collision hazard due to meteoroids of mass within the photographic range at a position in Earth's orbit, but far from Earth. Use was made of previously developed weighting factors to correct for biases in the photography of meteors. These biases were caused by meteoroid mass and velocity and the direction in space from which a meteoroid comes. The analysis was based upon data for photographic meteors supplied by the Smithsonian Astrophysical Observatory.

A damage criterion supplied by Ames Research Center was used; it contained as factors the normal component of impact velocity to the 0.875 power and particle mass to the 19/54 power.

The analysis showed a substantial advantage in (1) orienting a plane sheet of armor normal to the apex of Earth movement, (2) orienting a cylindrical tube in a direction with one end of its axis pointing toward the Sun, and (3) arrangement of a panel of tubes, with one end of the axis of each pointing toward the Sun, all in a plane normal to the apex of Earth movement. However, the relative advantages of orientation would rapidly change with changes in the ratio of the exponents of mass and velocity in the damage criterion used, possibly even to the extent of reversing.

Bimodal log-normal equations were obtained and integrated for normal components of impact velocity on planes, cylinders, and spheres with three principal orientations of the planes and cylinders. Necessary armor thicknesses for a desired probability of no destructive impact were determined with a double integration of particle mass and velocity so that all possible combinations of mass and velocity were taken into account.

Implications are found and discussed to the effect that a tentative description of the total meteoroid population of the solar system can be derived, from various characteristics of the sample existing in Earth's orbit. By similar methods, the overall meteoroid hazard could be estimated for an interplanetary mission.

INTRODUCTION

Meteoroids, small particles moving in orbit about the Sun, constitute a hazard to various components of space vehicles. Space radiators that might be required for a long mission are particularly vulnerable to destructive impact. Such radiators, used for rejection of waste heat from powerplants,, would need to be large because their effectiveness would be based entirely on radiation of heat to space, not including any effect of conduction and convection as with land-based powerplants.

A necessary step in calculation of the hazard from meteoroids has been determination of the flux rate relative to mass and of the velocity distribution for a given mass, because the greater the mass or the velocity of a meteoroid impacting upon a metal surface, the greater the damage.

Meteoroids that have relatively high probability of destructive impact upon space radiators are those within the so-called photographic range of mass. When such a meteoroid encounters the atmosphere of Earth, ablation or rapid erosion occurs with much luminous radiation. The result is a streak, known as a *meteor*, having sufficient luminous energy to permit photography from the ground.

As explained in reference 1, prior to the work reported therein, other investigators had advanced meteor theory to a point such that relative values of mass and absolute values of velocity, orbital parameters, and other characteristics of the particle that caused a given meteor could be well determined. (Absolute values of mass are still somewhat uncertain.) Difficulties still existed because of important biasing effects in the photographic process caused by (1) meteoroid mass, (2) meteoroid velocity relative to Earth's atmosphere, and (3) zenith angle (angle of the meteor path through the atmosphere to the zenith). An additional spatial bias existed because of the necessary location of the cameras in a fixed position (New Mexico) rather than in positions randomly varied over Earth's surface, the necessity of operation of the cameras exclusively at night, and the operation of the cameras principally during the later hours of the night.

Weighting factors to correct the various biases were developed and well confirmed in the work reported in references 1 to 5. With use of these weighting factors, velocity distributions without regard to direction of impact were determined both relative to a hypothetical gravity-free Earth and relative to the real Earth. Log-normal equations were developed representing both velocity distributions closely.

Also, the equation for meteoroid influx relative to mass from reference 6 was well confirmed throughout the photographic range. A double integration for meteoroid damage was performed with use of (1) any specified frequency function for velocity (velocity distribution), (2) the mass influx equation, and (3) a generalized equation for use with any damage criterion provided such criterion is proportional to the product of some power of mass and some power of impact velocity.

In the work reported here, the weighting factors were used in determining the distribution of normal components of impact velocity on spheres and on planes and cylindrical surfaces oriented in the three principal manners relative to the ecliptic plane and the apex of Earth movement (the momentary direction of Earth's movement). Log-normal equations for velocity distribution and sample calculations of necessary armor thickness are included. As in the earlier work, use was made of data from reference 7, which were provided on punched cards by Smithsonian Astrophysical Observatory.

Attention will be given to the bearing of the results of the analysis on the possibility that the meteoroid population at any desired position in the solar system may be tentatively deduced.

METHOD OF PROCEDURE

Distributions of normal component of impact velocity in the form of histograms were constructed for surfaces of structures traveling in Earth's orbit about the Sun but assumed to be far enough from Earth that impacting meteoroids would be negligibly affected by Earth's gravity. Three basic structural forms were included: (1) a sphere, (2) a plane, and (3) a cylinder having infinite ratio of length to diameter. For the plane and the cylinder three orientations were included as is illustrated in sketch (a) below.

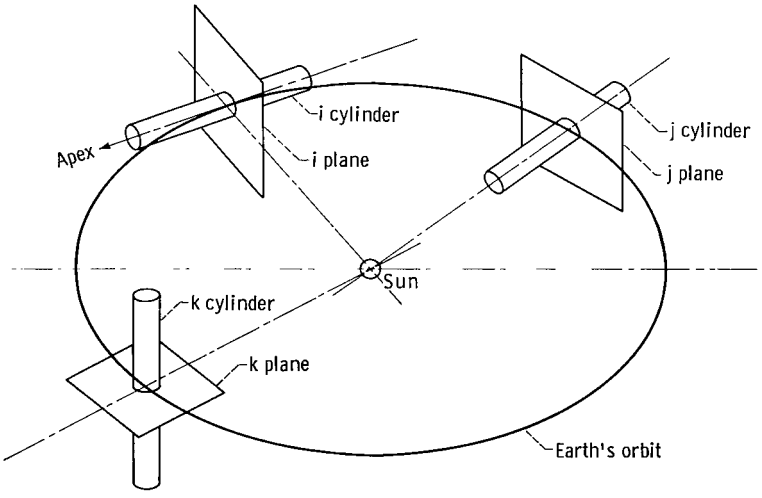

(a)

An axis normal to the plane, or the axis of the cylinder, was alined with positive direction as follows: (1) pointing in the direction of Earth movement in its orbit (i orientation), (2) pointing in a direction approximately away from the Sun, but exactly perpendicular to the i orientation and within the plane of the ecliptic (j orientation), and (3) pointing in a direction normal to the ecliptic plane southward (k orientation). A description of the method of computing data on distributions of normal velocity components for use in constructing the histograms just discussed, with reference to several appendixes, will constitute the first major section of this presentation.

Log-normal equations were developed to represent at least approximately the distribution of normal velocity component shown by each histogram. A description and discussion of these equations will be a second principal section of the presentation.

A third section will deal with computation of a concentration factor φ_g for each orientation of a plane or a cylinder, representing the frequency of impacts as compared with the expected frequency for a similar structure randomly oriented.

The fourth principal section will present sample computations of necessary armor thickness for the structures and orientations treated. Quantitatively, these computations will not be intended as a definitive result. They will, however, demonstrate a method that is generally applicable with a wide variety of damage criteria that might be selected and they will provide a comparison of the effectiveness of the various orientations of the structures studied. The computations will use the log-normal distribution equations and the values of φ_g in the manner described in reference 4. The sample calculations required integration of the log-normal velocity distributions to allow construction of curves representing the average value of the n^{th} power of the normal component of impact velocity $\overline{v_{norm}^n}$ (where v_{norm} is the normal component of impact velocity and n is any arbitrary positive number).

The fifth principal section, and the last preceding a general discussion of results, will be concerned with the possible bearing of the study on the general meteoroid population of the solar system.

COMPUTATIONS FOR USE IN CONSTRUCTION OF HISTOGRAMS OF NORMAL VELOCITY COMPONENTS

Distributions of normal components of impact velocity were obtained as weighted counts of sporadic meteors within each of 80 velocity classes with use of a computer program. Each class had a central value (class mark) of an integer plus one-half, from 1/2 to $79\frac{1}{2}$ kilometers per second (km/sec). Thus, each velocity class extended throughout a range of 1 km/sec. The sporadic meteors used for the weighted count were a por-

tion of those for which data were published in reference 7. They were chosen in a manner that will be explained later. For explanation of the method of making the weighted count, it is convenient to use the concept of an adjusted unit count, which will now be explained.

Adjusted Unit Count

For determination of an adjusted unit count, the weighting factor developed in references 1 to 5 was used.

$$\varphi_w = (\cos Z_R)^{-0.22} F(Z_R)_{av}^{0.712} v_\infty^{-3.87} \varphi_s \quad (1)$$

As was explained in those references, the correct distributions of velocity or various other parameters should be obtained if each meteor is counted, not as one meteor, but as φ_w meteors. That is, φ_w may reasonably be termed an "adjusted unit count" for statistical purposes.

In the right-hand side of equation (1), $\cos Z_R$ is cosine of the zenith angle, or angle between the path of the meteor and the zenith (CZ_R of ref. 7). The symbol v_∞, as in reference 7, represents the velocity of the meteoric particle relative to Earth's atmosphere before any deceleration by resistance of the atmosphere. The symbol $F(Z_R)_{av}$ represents a statistically expected value of a function of zenith angle, position of the meteor within the camera field of view, and azimuth of the meteor path, which was calculated and recorded for each meteor as part of the work described in reference 1. The value of $F(Z_R)_{av}$ is concerned with the density of the meteor trace on the photographic plates. The values recorded in the work of reference 1 were used here in equation (1). The value of φ_s is a spatial weighting factor, inverse values of which were calculated in the work described in reference 5. It is concerned with the probability that a meteor would reach the atmosphere over the camera sites in New Mexico during the times at which the cameras were operated, in consideration of the direction in space from which it came and in consideration of its geocentric velocity. The probability φ_s for a meteor is not absolute, but is correctly related to the value of φ_s calculated for any other meteor. (In general, the significance of any symbol used in this report is explained in appendix A.)

To obtain data for the desired histograms, the adjusted unit count was applied to the meteors that were selected for use. Orbital data given in reference 7 were used to derive components of meteor velocities normal to the surfaces of the structures that were under study. The adjusted unit counts, or fractions of them, corresponding to a given

class of normal velocity component were added to produce an adjusted total for that normal velocity class. The types of meteors included in the analysis, the types of orbits treated, simplifying approximations made, the orbital parameters used, and certain needed basic constants will be discussed before the method of resolution of velocities is begun.

Meteors Used for Determination of Velocity Distributions

Of the sporadic meteors reported in reference 7, 1282 were used, as in reference 4. All rejections of sporadic meteors were for two reasons:

(1) To avoid unrealistic values of the adjusted unit count φ_w of equation (1) meteors having a value of $\cos Z_R$ less than 0.2 were rejected. The manner of calculation of the inverse value of φ_s in the work of reference 5 included a provision to eliminate any statistical bias that might be introduced by these rejections.

(2) Meteors were rejected if, at the time of impact, the meteoric particles were approaching the ecliptic plane from the south or if the components of their velocities approximately in the direction away from the sun and exactly perpendicular to the apex of Earth movement were positive. This provision, as explained in reference 4, confined the sample of meteoroids to a quadrant of the space surrounding Earth that could be completely covered; that is, at some periods during the operation of the cameras, meteors of any velocity could be photographed from any direction whatever lying within that quadrant. Restriction of meteors to that quadrant, as explained in reference 4, was based on an assumption of two planes of symmetry for approach of meteoroids toward Earth.

Orbital Types and Simplifying Approximations

A decision was made to use the equations for each of the three conic sections, ellipse, parabola, and hyperbola. Use of the three sections involved no decision on the controversial question as to whether parabolic or hyperbolic orbits actually exist. The data as presented in reference 7 indicate such orbits, and, even though such indication may well be due to inaccuracy of the data reduction, no rule could be set by which the given data could be warped to form elliptical orbits without the danger of introducing even greater inaccuracy.

Hyperbolic orbits in reference 7 were indicated by negative values of a (semi-major axis, in case of ellipse) and the absence of values of q' (aphelion). The negative values were compatible with the other parameters given when made positive (for later purposes)

and used in the basic equation of a hyperbola

$$\frac{x^2}{a^2} - \frac{y^2}{b^2} = 1 \tag{2}$$

Parabolic orbits were indicated by absence of values of both a and q', with eccentricity e equal to 1.00. The indication of a parabolic orbit is equivalent to an indication that the heliocentric velocity v_H is equal to the velocity of escape from the Sun. The values of v_H given in reference 7 for the few cases of parabolic orbits were not identical, possibly because of difference of the Earth's distance from the Sun. In this analysis, a satisfactory degree of accuracy was possible with substantial simplification of the computations by treating the Earth's orbit as exactly circular with a radius of 1 astronomical unit. Accordingly, for the parabolic orbits a calculated velocity of escape was substituted for the given value of v_H in each case. For elliptical and hyperbolic orbits the value of v_H (from ref. 7) was used.

Orbital Parameters Used for Each Meteor

Because of redundancy, parts only of the data presented for each meteor in reference 7 were used. Certain checks were made on the consistency of the unused data with the data that were used. Details are presented in appendix B.

Basic Constants

Certain basic constants needed in the resolution of velocities are explained in appendix C. Derivations are included for the less obvious constants.

Determination of Three Principal Components of Meteoroid Velocity Relative to Gravity-Free Earth

As a first step in determining normal components of impact velocity of a meteor upon the structures under consideration, a vector representing heliocentric velocity $\overrightarrow{v_H}$ was resolved into components extending in three directions: (1) the i direction, toward the apex of Earth movement in its orbit (positive for meteoroids in direct motion, negative for meteoroids in retrograde motion), (2) the j direction, within the plane of the

ecliptic, approximately in the direction away from the Sun, but exactly perpendicular to the apex of Earth movement (negative for all meteoroids treated), and (3) the k direction, normal to the ecliptic plane and southward (positive for all meteoroids treated). Such preliminary resolution of the velocity $\vec{v}_H$ is explained in detail in appendix D. Next, as also explained in appendix D, three similarly directed components of velocity were determined, but for the vector velocity $\vec{v}_G$ relative to the moving Earth rather than for the velocity $\vec{v}_H$ relative to the Sun.

Determination of Velocity Components Normal to Surfaces of Structures from Principal Components of Velocity Relative to Earth

Two of the components of $\vec{v}_G$, namely, $\vec{v}_{jr}$ and $\vec{v}_{kr}$ from equations (D43) and (D44), were usable directly as normal components of impact velocities upon planes with the j and k orientations. Because of an assumption of symmetry relative to both the k and j planes, it was convenient and permissible to make the values of these components arbitrarily positive. The third component, $\vec{v}_{ir}$ from equation (D42), was usable directly as a normal component of impact velocity on a plane with i orientation. But here symmetry did not exist. If $\vec{v}_{ir} \cdot \vec{i}$, with $\vec{v}_{ir}$ as given by equation (D42), was negative, impact occurred on the leading side of the plane. If that value was positive, impact was on the trailing side.

Normal components of impact velocity on different parts of the surfaces of cylinders with i, j, and k orientations were readily determined with use of the vector components $\vec{v}_{ir}$, $\vec{v}_{jr}$, and $\vec{v}_{kr}$. The sum of the three vector components could have been used for determination of the normal component of impact velocity on various parts of a sphere. But, as a sphere presents the same shape, size, and relative orientation of vulnerable surface toward a meteoroid that approaches from any direction, the scalar value v_G as given in reference 7 was usable directly.

The details of the determination of normal components of impact velocity on various parts of the surfaces of cylinders and spheres are explained in appendix E.

Normal Velocity Distributions as Normalized Sums of Adjusted Unit Counts

The circular symbols in figures 1 to 3 represent histograms. To avoid unnecessary confusion, the usual vertical bars of histograms are omitted. The circular symbols correspond to the tops of those bars. The curves, representing the general trend of the circular symbols, will be discussed in a later section. Effectively, the datum used for

plotting each circular point was a normalized sum of adjusted unit counts for all meteoroids that would impact upon the pertinent structure (sphere, plane, or cylinder), with the pertinent orientation of that structure, with a normal component of impact velocity within the pertinent velocity class. The summation for each velocity class included only a part of each adjusted unit count. Such part of the adjusted unit count was equal to the total adjusted unit count (eq. (1)) multiplied by a relative probability that the particular meteoroid under consideration would impact the structure with normal velocity component within the pertinent velocity class. That relative probability consisted of two factors. For definition of factor (1), consider a great number of hypothetical meteors, all exactly like the particular meteor under consideration and all impacting the given structure with the given orientation. Then factor (1) is the fraction of those hypothetical meteors that would impact with a normal component of impact velocity within the velocity class under consideration. Factor (2) is the vulnerable area presented to the given meteoroid by the given structure with the given orientation, measured as a projected area upon a plane normal to the path of the meteoroid. For planes, factor (1) for a given meteoroid was unity for one velocity class and zero for all others. For spheres and cylinders, factor (1) was nonzero for all velocity classes up to a maximum value of velocity. Sums of adjusted unit counts for the different velocity classes were finally normalized by dividing each of the sums by the total of all of them. Hence, factor (2) could be applied without reference to any particular standard size of structure so long as the dimensions of the structure were kept constant. The methods involved in obtaining the normal velocity distributions as normalized sums of adjusted unit counts are described in detail in appendix E.

LOG-NORMAL EQUATIONS FOR DISTRIBUTION OF NORMAL COMPONENT OF IMPACT VELOCITY UPON PLANES, CYLINDERS, AND SPHERES

In figures 1 to 3, curves have been constructed to represent unimodal or bimodal offset log-normal equations. Each triangular plotted symbol represents the result of a calculation, with use of the pertinent equation, for the percentage of all impacts having a normal component of impact velocity at the given value of the abscissa ±0.5 km/sec. The curved line was drawn through the triangular points as guides.

In each part of each figure, the equation represented is of the form

$$f(v_{norm}) = \sum_{i=1}^{2} C_i \exp\left\{-\frac{1}{2}\left[\frac{\ln (v_{norm} + \delta_i) - \mu_i}{\sigma_i}\right]^2\right\} \quad (3)$$

in which $f(v_{norm})$ is the fractional frequency of occurrence of a given value of v_{norm} ± 0.5 km/sec (multiplied by 100 for plotting in the figures). The offset δ_i is arbitrarily equal to zero for $i = 2$. The constants C_i, μ_i, and σ_i, as well as δ_i with $i = 1$, may be varied independently to improve the fit of the resulting curves to the velocity histograms (circular symbols in figures).

An equation of such form was found in reference 4 to provide a good representation of the gross impact velocities for both near-Earth and far-from-Earth (real Earth and gravity-free Earth) conditions. For figures 1 to 3, the constants of equation (3) were varied in a trial-and-error procedure to fit the equation as well as possible to the histograms. The resulting values of the constants are shown in table I.

In four cases the fit of the curves to the histograms is so good, with due regard for the random vertical scatter of the data, that search for a better equation would not appear to be justified. Those cases are figure 1 (a, b, and c) and figure 2(c), with a minor exception for figure 1(b) that will be discussed later. The four cases cover the leading and trailing sides of the i plane, either side of the j plane, and the k cylinder. In all other cases, the fit is obviously not perfect, though in each case it was the best that could be obtained with use of equation (3). Improvement could be effected with much labor by adding one or more terms to equation (3), that is, by varying i from 1 to 3,

TABLE I. - VALUES OF CONSTANTS IN OFFSET BIMODAL LOG-NORMAL EQUATION TO PROVIDE BEST APPROXIMATION OF HISTOGRAM REPRESENTING NORMAL COMPONENT OF IMPACT VELOCITY ON STRUCTURES WITH VARIOUS ORIENTATIONS.

Structure	Coefficient in eq. (3)		Offset	Logarithmic modal value		Logarithmic standard deviation	
	C_1	C_2	δ_1	μ_1	μ_2	σ_1	σ_2
i plane (leading side)	0.1433	1.385×10^{-3}	0	1.100	3.90	0.700	0.200
i plane (trailing side)	.1880	0	25.0	3.420	----	.0692	-----
j plane	.0883	1.365×10^{-2}	5.0	2.560	3.05	.280	.225
k plane	.0947	2.808×10^{-3}	2.0	2.050	3.29	.470	.170
i cylinder	.0894	8.86×10^{-3}	2.0	2.080	3.04	.450	.225
j cylinder	.1220	2.910×10^{-4}	0	1.600	3.66	.560	.270
k cylinder	.0899	7.53×10^{-5}	2.0	2.050	4.00	.503	.120
Sphere	.0919	8.13×10^{-5}	2.0	2.010	3.96	.510	.115

1 to 4, and so on. In all cases, however, the author believes the fit of the curves to the histograms, with only the two terms, is good enough to provide reasonable accuracy by use of the equations.

In figure 1(b) four data points at $18\frac{1}{2}$, $26\frac{1}{2}$, $28\frac{1}{2}$, and $44\frac{1}{2}$ km/sec, were ignored in the fitting of the curve because (1) these points lie on such a low level on the ordinate scale it was believed their inclusion would have negligible effect on the end result of the analysis, (2) they are so widely scattered that they do not constitute an adequate sample upon which to base a second mode (i = 2) for equation (3), and (3) the probability is high that the data points appear in the figure only because of error.

The $18\frac{1}{2}$-km/sec point was caused by meteor 3005 (p. 44, ref. 7); the $26\frac{1}{2}$-km/sec point by meteor 11178 (p. 48); the $28\frac{1}{2}$-km/sec point by meteors 4424 and 6977 (p. 67, and p. 42); and the $44\frac{1}{2}$-km/sec point by meteor 3204 (p. 47). Heliocentric velocities v_H given for these five meteors are 66.1, 83.0, 81.7, 61.2, and 77.9 km/sec. These velocities correspond to hyperbolic orbits as is clear from comparison with the 42.14-km/sec value (eq. (C6)) for a parabolic orbit, which is the boundary condition between elliptical orbits (particles permanently bound by the Sun) and hyperbolic orbits (particles arriving from or at least permanently departing for the space outside the solar system).

If the heliocentric velocities reported for these meteors were erroneous by at least the amounts they exceed 42.14 km/sec, the errors were great even for the graphical method used for the results reported in reference 7. Nevertheless R. E. McCrosky (of ref. 7) emphasized in a personal communication that a hyperbolic orbit for a meteor has never been confirmed when the data were subjected to precise reduction, and he thinks it unlikely that any of these five apparent hyperbolic orbits would be confirmed.

Particles in hyperbolic orbits (correctly or not) affect all the histograms in figures 1 to 3 and affect that in figure 1(b) in the regions below $18\frac{1}{2}$ km/sec as well as at that velocity and above. But, except in figure 1(b), and only for the higher velocities there, no serious error results. An occasional multiplication of a correct nonzero frequency by a factor of 2 or 3 on the logarithmic scale of ordinates, because of a falsely high value of v_H, is no more serious than the random scatter that is apparent in all parts of the histograms.

CONCENTRATION FACTORS FOR FREQUENCIES OF METEOROID IMPACT UPON VARIOUSLY ORIENTED STRUCTURES

In reference 4 a method was set forth for computing necessary armor thickness for a space mission to provide a specified low probability of avoidance of disastrous impact. Application of that method here will require the use of equation (3) with the values of constants shown in table I. It will also require, for each orientation of each structure,

TABLE II. - TOTAL IMPACTS ON PLANES, CYLINDERS, AND SPHERES AS PERCENTAGES OF EXPECTED IMPACTS ON RANDOMLY ORIENTED SURFACES.

Structure and orientation	Total impacts, $\varphi_g \times 100$
i oriented plane (leading side)	31.10
i oriented plane (trailing side)	122.30
j oriented plane, either side alone	121.07
k oriented plane, either side alone	91.26
i oriented cylinder	110.30
j oriented cylinder	85.01
k oriented cylinder	101.78
Sphere (in effect, randomly oriented surface)	100.00

a concentration factor φ_g as used earlier in reference 4. That factor may be defined as the ratio of the frequency of impacts upon the structure to the expected frequency of impacts upon one side of the same surface area when randomly oriented.

Calculations of the concentration factor φ_g are explained in appendix F. The results are tabulated in table II as percentages.

SAMPLE COMPUTATIONS OF ARMOR THICKNESS FOR PROTECTION FROM METEOROIDS

In reference 4 a method of computation that will be used here was presented and explained for determining the necessary armor thickness to provide a desired high probability of encountering no disastrous impact by a meteoroid during a space mission. Neither the sample computations in reference 4 nor those here are intended to provide a definitive result. In particular, the computations do not include any consideration of shower associated meteoroids, which would require further study. The computations are intended as a demonstration of a method that may be applied to various possible damage criteria as well as to a specific damage criterion used as an example. Also, the results here will serve as an illustration of the effect of structure orientation as governed by a specific criterion and will indicate qualitatively how the effect of orientation might change with use of other damage criteria.

As in reference 4, a space mission will be assumed with a duration of 1000 days, and the specific damage criterion used will be

$$t_{cr} = 0.8162\,\epsilon_t^{-1/18}\rho_p^{8/54}\rho_t^{-1/2}m^{19/54}v_{norm}^{0.875} \tag{4}$$

in which t_{cr} is minimum armor thickness (cm) at which penetration would occur, ϵ_t is percent elongation of armor material, ρ_p is density (g/cm^3) of particle, ρ_t in density (g/cm^3) of armor material, m is mass (g) of particle, and v_{norm} is the normal component of impact velocity (km/sec). Equation (4) represents a formula provided by Richard H. Fish and James L. Summers of Ames Research Center in a personal communication. As in reference 4, stainless steel armor will be assumed with values of ρ_t equal to 8 grams per cubic centimeter and ϵ_t equal to 10 percent. Meteoroid density ρ_p will be taken as 0.2 gram per cubic centimeter.

In reference 4, the critical armor thickness necessary under the conditions specified and with use of equation (4) was, in effect, found to be

$$t_{cr} = 0.200\left\{\frac{3.287\times10^{-15}\,TA\left[\varphi_g v_{norm}^{(1.34\,\epsilon/\lambda)}\right]}{p}\right\}^{\lambda/1.34} \tag{5}$$

where T is the duration of the mission in seconds, A is vulnerable area in square meters, p is average number of destructive impacts expected per mission (very closely equal to the complement of the desired probability of no destructive impact when that desired probability is high), ϵ is the exponent of v_{norm} in an equation such as (4), and λ is the exponent of m in the same equation. The symbol φ_g was used in reference 4 with the same significance as here. The derivation of equation (5) involved a double integration relative to a well confirmed mass distribution and the velocity distribution shown by equation (3), so that impacts by meteors of all masses and all values of v_{norm} are involved in the solution. However, it was found that the result (eq. (5)) is usable for any velocity distribution.

Equation (5) is simply a rearrangement of an equation that was derived in reference 4, which was linear in a variable Z_{cr}. The critical thickness t_{cr} in equation (4) is a specific case for the general variable Z_{cr} of reference 4. Now, let it be supposed that we might wish to use two or more expressions for t_{cr} similar to equation (4), each applicable only within a specific range of values of v_{norm} and each having its own values of ϵ and λ, that is, ϵ_1 and λ_1 for the first expression, ϵ_2 and λ_2 for the second expression, and so on. Then, by the same method used in reference 4, we could easily derive a nonlinear equation in t_{cr} analogous to equation (5). With n equations like equation (4), for n different ranges of v_{norm} value, the nonlinear equation in t_{cr} would contain n terms in t_{cr}, in which the symbol t_{cr} would be raised to n different

powers (integral or nonintegral). The nonlinear equation would also include averages of n different powers of v_{norm} and each average would be taken only over the pertinent range of v_{norm} value. Such nonlinear equation could be solved for the critical value t_{cr} by approximate methods. Although multiple roots would exist, physical reasons would also exist for excluding all roots but one.

Substitution of numerical values in equation (5) yields

$$t_{cr} = 0.003818\left(\frac{A\varphi_g\overline{v_{norm}^{3.332}}}{p}\right)^{0.2626} \tag{6}$$

In reference 4, methods were derived for integration of equation (3) under certain conditions to yield an average value $\overline{v_{norm}^{n}}$. Under other conditions, recourse must be made to direct numerical integration. Use of those methods, including direct numerical integration, with the constants shown in table I, produced the values of $\overline{v_{norm}^{n}}$ shown in figures 4 to 6, for planes, cylinders, and spheres, with the various orientations that have been discussed for planes and cylinders.

Thicknesses of armor necessary for certain probabilities of no destructive impact and certain vulnerable areas were computed with use of equation (6) for planes and cylinders, with the three principal orientations, and for spheres. Values of $\varphi_g\overline{v_{norm}^{3.332}}$ were taken from the integration results plotted in figures 4 to 6. The resulting armor thicknesses, with pertinent data, appear in table III.

TABLE III. - COMPUTED THICKNESSES OF ARMOR NECESSARY FOR PROTECTION FROM METEOROID IMPACT UNDER SEVERAL SETS OF CONDITIONS OVER A PERIOD OF 1000 DAYS

Structure	Orientation	Vulnerable area		Approximate probability of no destructive impact, percent	Average number of destructive impacts per mission (p in eq. (6))	Value of φ_g from table V	Value of $\varphi_g\overline{v_{norm}^{3.332}}$	Critical thickness by equation (6)	
		ft^2	m^2					in.	cm
Plane	i (leading	1000	92.9	99.5	0.005	0.311	7745	0.209	0.530
		500	46.5	99.75	.0025	.311	7745	.209	.530
	i (trailing)	1000	92.9	99.5	.005	1.223	661.9	.109	.278
		500	46.5	99.75	.0025	1.223	661.9	.109	.278
	j	2000	185.8	99.0	.01	1.211	11 695	.232	.590
		1000	92.9	99.5	.005	1.211	11 695	.232	.590
	k	2000	185.8	99.0	.01	.913	6204	.197	.500
		1000	92.9	99.5	.005	.913	6204	.197	.500
Cylinder	i	2000	185.8	99.0	.01	1.103	8752	.215	.547
	j	2000	185.8	99.0	.01	.850	5379	.190	.481
	k	2000	185.8	99.0	.01	1.018	7243	.205	.521
Sphere		2000	185.8	99.0	.01	1.000	6310	.198	.502

IMPLICATIONS REGARDING TOTAL METEOROID POPULATION OF SOLAR SYSTEM

A possibility exists that the meteoroid population of the solar system may possess interrelations necessitated by the effects of collisions between different meteoroids. These interrelations might be analogous to those existing between the molecules of a gas in a container. Although the collisions of meteoroids would of course be far from elastic, some changes in momentum components would occur upon collision and some kind of randomization of the motion should result.

The frequency of collision for a given size of particle may be estimated with equations presented in reference 4, of which equations (4) and (5) are specific forms. The general equations are

$$Z = C_3 m^{\lambda} v^{\epsilon} \tag{7}$$

and

$$Z_{cr} = C_3 \left[\frac{3.287 \times 10^{-15} \, TA\left(\varphi_g \overline{v^{1.34\,\epsilon/\lambda}}\right)}{p} \right]^{\lambda/1.34} \tag{8}$$

where Z is any damage criterion, Z_{cr} is a critical value of Z, C_3 is a constant, and v is an impact velocity of the applicable type.

Now consider a particular spherical meteoroid of mass 10^{-3} gram and a density of 0.2 gram per cubic centimeter (see, e.g., ref. 8 as source of density chosen). Assume the meteroid is moving about the Sun in the same orbit as the Earth. Let us estimate the time required for a 50-percent probability of at least one impact with another meteoroid of the same or greater mass.

The radius of the meteoroid would be 0.106 centimeter. However, for impact with a similar meteoroid, its effective vulnerable area would be multiplied by four. In effect, its radius (i.e., the total distance between centers of two meteoroids in contact) would be doubled. The vulnerable area, then would be 0.1414 square centimeter, facing an approaching meteoroid from any direction. The corresponding total external vulnerable area of the sphere (A of eq. (8)) would then be 0.5656 square centimeter (or 5.656×10^{-5} m^2).

Now as any collision with a meteoroid of mass greater than 10^{-3} gram is to be considered, the criterion Z in equation (7) is just the mass m. Hence,

$$\left.\begin{aligned} C_3 &= 1 \\ \lambda &= 1 \\ \epsilon &= 0 \end{aligned}\right\} \tag{9}$$

and in equation (8), $Z_{cr} = 10^{-3}$; that is, the critical mass m to be considered. For a 50-percent probability of no impact within the specified mass range, according to the Poisson distribution, the value of p in equation (8) should be $p = -\ln 0.5 \approx 0.6931$.

As the total vulnerable area is the surface of a sphere, in effect a randomly oriented surface, $\varphi_g = 1$. So, equation (8) becomes

$$10^{-3} = \left[\frac{3.287\times10^{-15} \times 5.656\times10^{-5}\ T}{0.6931}\right]^{1/1.34} \tag{10}$$

and

$$T = 3.56\times10^{14}\ \text{sec} = 1.129\times10^{7}\ \text{yr} \tag{11}$$

The time is indeed long, but very short in comparison with the age of the solar system. Moreover, collisions with smaller meteoroids would be many times more frequent. Therefore, it seems reasonable to assume that nearly all meteoroids have undergone numerous collisions. Great heat would be generated, the resulting thermal explosions should release much gas, which presumably would become part of the solar wind and escape from the solar system. Any solid residue should be expected to be solidified froth (because of the expansion of hot bubbles of gas within it while in the molten state). Such condition would explain the low density of 0.2 gram per cubic centimeter. But, most importantly, the residual particles should move in random directions relative to the average direction of motion of particles in Earth's orbit.

Figures 4 to 6 are interesting to examine relative to this collision hypothesis. It is obvious at once from figure 4 that the total flux of kinetic energy is at least approximately the same in both directions through the i plane, because the values of $\varphi_g \overline{v^2_{norm}}$ are the same for the two sides of this plane. (It was shown in refs. 2 and 3 that the velocity of meteoroids is statistically independent of mass.) It is equally obvious that the flux of momentum (proportional to $\varphi_g \overline{v_{norm}}$) is substantially greater for the trailing side of the i plane than for the leading side.

Now consider the levels at $n = 4$ for curves that might be drawn through the four

sets of plotted values of $\varphi_g \overline{v^n_{norm}}$ in figure 4. For the leading side of the i plane, the level at n = 4 would be about 1.1×10^5 with $\varphi_g = 0.311$. For the trailing side of the same plane, the level would be about 2.7×10^3 with $\varphi_g = 1.223$. The average value, $\overline{v^4_{norm}}$, for both sides of the i plane, then, would be the sum of these values of $\varphi_g \overline{v^4_{norm}}$ divided by the sum of the two values of φ_g or about 7.3×10^4. The level for the j plane from the figure is about 9.4×10^4 with $\varphi_g = 1.2107$, so that the value $\overline{v^4_{norm}}$ should be about 7.8×10^4. For the k plane, the value of $\varphi_g \overline{v^4_{norm}}$ would be about 5.6×10^4 with $\varphi_g = 0.9126$, so that $\overline{v^4_{norm}}$ should be about 6.1×10^4. Now it is seen that the three values, 7.3×10^4, 7.8×10^4, and 6.1×10^4, are the same within a logarithmic range of about 0.11.

The three curves in figure 5 would yield about the same results. Although these curves are for normal impact velocity on the surfaces of cylinders, each of them is equivalent to the average n^{th} power of component of impact velocity on the family of planes passing through the axis of the pertinent cylinder. In figure 6, the curve for normal components of impact velocity on a sphere (equivalent to a randomly oriented plane) passes through approximately the same level at n = 4 as do each of the three curves of figure 5.

Now, if we disregard particle mass because it is independent of velocity, the value $\overline{v^4_{norm}}$ is proportional to the variance (square of the standard deviation) of kinetic energy. This variance relates to a zero value of kinetic energy (v = 0). In statistics, in a manner analogous to mechanics, the variance of v is known as the second moment of v. As in mechanics, the first moment becomes zero if recomputed in relation to its own value as a base. As with the second moment in mechanics (moment of inertia), the second moment can be corrected relative to a base equal to the value of the first moment simply by subtracting the square of the value of the first moment.

Such a correction on the values of $\overline{v^4_{norm}}$ obtainable from figures 4 and 5, with use of the base values of $\overline{v^2_{norm}}$ that can be obtained in those figures, would produce very little change. Hence, the same level of $\overline{v^4_{norm}}$ for all the curves at n = 4 in figures 4 to 6 is a direct demonstration that the standard deviation of kinetic energy is the same for the velocity components in all directions. This observation, together with the earlier mentioned observation from figure 4 (the equivalence of flux of kinetic energy from the two directions through the i plane), suggests that possibly the flux of kinetic energy should really be the same through all planes. The failure of figure 4 to show this fact at n = 2, then, could be due to the use of the wrong base value for v_{norm} for the j and k planes. That is, possibly the j and k planes should be treated as moving relative to Earth. If they should be treated as moving southward and toward the Sun, then treating them as stationary relative to the Earth as has been done in this analysis would cause the flux of kinetic energy to appear too high through the j and k planes. This effect

would exist because this analysis was limited to meteors that approached the j plane from the antisolar direction and approached the k plane from the north.

It is beyond the scope of this report to develop a kinetic theory for the highly inelastic collision of high-velocity particles in a vacuum to show that the flux of kinetic energy should be invariant with orientation of the axes, even though the flux of momentum and flux of particles are both clearly not so. The purpose here is merely to examine the implication of that hypothesis, which has been suggested by the observations that have just been discussed.

It is reasonable to assume that the average flux of kinetic energy of meteors through the Earth's orbit has components southward through the ecliptic plane and inward toward the Sun. Such a flux would have to be compensated by outward and northward flux at other distances from the Sun. The suggestion of such a toroidal flux is not new (see, for example, the discussion of toroidal meteors in ref. 9). (This assumption, of course, at least partly contradicts the assumption of symmetry upon which was based much of the work reported here.)

The effect of assumed movement of the j and k planes southward and sunward will now be examined. (The consequent modification of observed flux frequencies could be computed in a repetition of the entire analysis presented here, but this modification will be neglected at this time.)

In figure 4, the ordinates at $n = 2$ for the two sides of the i plane will be assumed correct. Any attempt to modify them by assuming that the i plane should be moving relative to the Earth would only shift one of them upward and the other downward, defeating the concept of equal flux of kinetic energy in any direction. So to equate the fluxes of kinetic energy for the three planes, it will be necessary to move the ordinates at $n = 2$ for the j and k planes downward to match those of the i plane.

For the j plane, the value of $\varphi_g \overline{v^2_{norm}}$ from figure 4 is about 204. With $\varphi_g = 1.2107$, the corresponding value of $\overline{v^2_{norm}}$ is about 170. The value of $\varphi_g \overline{v_{norm}}$ is about 14.8, so that $\overline{v_{norm}}$ is about 12.2. The value of $\overline{v^2_{norm}} = 170$ is the second moment of v_{norm} relative to the base value $v_{norm} = 0$. In the same manner as used earlier it can be converted to the base $v_{norm} = 12.2$ simply by subtracting the square of that value, so that $\overline{v^2_{norm(12.2)}} = 18.4$.

For the i plane, the value $\varphi_g \overline{v^2_{norm}}$ is about 45. For the adjusted value of $\varphi_g \overline{v^2_{norm}}$ of the j plane to match this value, neither $\overline{v^2_{norm}} = 170$ nor $\overline{v^2_{norm(12.2)}} = 18.4$ will do. Instead, some base value v_b is needed such that $\varphi_g \overline{v^2_{norm(b)}} = 45$, where $v_{norm(b)}$ is the normal velocity component relative to the base v_b. With $\varphi_g = 1.2107$, then, $\overline{v^2_{norm(b)}} = 37$. Now, by the inverse of the process that was used before, the value $\overline{v^2_{norm(12.2)}} = 18.4$ can be converted to $\overline{v^2_{norm(b)}} = 37$ by adding $(v_b - \overline{v_{norm}})^2$. So,

$$\overline{v^2_{norm(b)}} = \overline{v^2_{norm(12.2)}} + (v_b - \overline{v_{norm}})^2 \tag{12}$$

or

$$37 = 18.4 + (v_b - 12.2)^2 \tag{13}$$

and

$$v_b = 12.2 \pm 4.3 \tag{14}$$

This result means that, for equating fluxes of kinetic energy between planes j and i, the average velocity component $\overline{v_{norm}}$ relative to the moving plane j must be approximately ∓ 4.3 km/sec rather than the value 12.2. The j plane, then, would need to be moving toward the Sun at either 16.5 or 7.9 km/sec. The value of $\varphi_g \overline{v_{norm}}$ would become 5.2 km/sec. As symmetry of velocity components v_{norm} relative to the j plane would now be assumed, the minus values of v_{norm} would amount to a reversal of flux direction, and the consequent modification of observed influx rates would be extreme. Hence, the sunward movement of the j plane at 7.9 km/sec will be chosen for use, with the reservation that it should probably be much reduced if the modification of observed influx rates had not been neglected. (To avoid reversal of flux, the smaller value of v_b must be used so that the southward movement of the meteoroids may still permit them to overtake the j plane.)

Now let us compare the momentum flux rate for the j plane, with $\varphi_g \overline{v_{norm}} = 5.2$ with that for the i plane. From figure 4, for the leading side of plane i, $\varphi_g \overline{v_{norm}} = 2.63$ with $\varphi_g = 0.311$. For the trailing side, $\varphi_g \overline{v_{norm}} = 7.6$ with $\varphi_g = 1.223$. The average value for the two sides of the i plane, then, is

$$\varphi_g \overline{v_{norm}} = \frac{2.63 + 7.6}{2} = 5.1 \tag{15}$$

This result is the same as the adjusted value of 5.2 for the j plane well within the probable accuracy of the determinations.

A similar analysis for the k plane showed that equalizing the flux of kinetic energy with that of the i plane would require an average velocity component normal to the moving k plane of 10.5 or 8.1 km/sec. For the same reason as before, the value 8.1 km/sec was chosen for movement of the k plane in the southward direction with a value of $\overline{v_{norm}} = 1.22$ km/sec relative to the moving k plane. The value of $\varphi_g \overline{v_{norm}}$

relative to the moving plane k, then, is $1.22 \times 0.9126 = 1.11$. This rate of southward motion of the k plane at 8.1 km/sec is probably much too high, because reduction of the average component of velocity from a value of about 9.3 derivable from figure 4 to the value 1.22 would mean a very substantial correction to the observed influx rate, that is, a substantial reduction of the factor φ_g. The large reduction in the factor φ_g would help to bring the kinetic energy flux for the k plane down toward that of the i plane without the need of assuming such a large velocity of southward motion for the k plane.

For the movement toward the Sun at 7.9 and southward at 8.1 km/sec the origin for the i, j, and k planes, moving at Earth velocity of 30 km/sec, would have to move at an angle equal to the arc sine of the expression

$$\sqrt{\frac{7.9^2 + 8.11^2}{30^2 + 7.9^2 + 8.11^2}}$$

or at an angle of about 21° to the apex of Earth movement. This result does not seem unreasonable, particularly in view of the fact it would be considerably reduced when taking into account the reduced frequency of observed impacts that would occur normal to the j and k planes because of the movement of those planes.

A rough check relative to existence of the toroidal flux was made. From a study of the results of the work of reference 5, it was estimated that the meteoroid sample of reference 7 would satisfactorily cover a solid angle defined by the spherical surface between two planes, both containing the apex and antapex of Earth movement. One such plane would extend through the apex-antapex line, away from the Sun, southward, at a dihedral angle of 44° to the ecliptic plane. The other plane would extend through the apex-antapex line northward and toward the Sun at a dihedral angle of 44° from the j plane.

Part of the computer program used in this study, as has been described, was repeated under two conditions: (1) with restriction of the sample to meteors arriving from the solid angle between two planes extending through the apex-antapex line, both away from the Sun, one northward and the other southward, at dihedral angles of 44° from the ecliptic, and (2) with restriction of the sample to meteors arriving from the solid angle between two planes extending through the apex-antapex line, both northward, one toward the Sun and the other away from the Sun, at dihedral angles of 44° from the j plane. The first result showed an average component toward the k plane (southward through the ecliptic) of 1.65 km/sec. The second result showed an average component of velocity toward the j plane (toward the Sun) of 2.18 km/sec. The component 2.18 km/sec toward the Sun is 27.6 percent of the value of 7.9 computed to equalize flux of kinetic energy. The value 1.65 km/sec is 20.3 percent of the value 8.11 computed as necessary

in the southward direction. The components equal to 1.65 and 2.18 km/sec would call for movement of the origin of the i, j, and k planes at an angle of only about $1/2^{o}$ to the apex of Earth movement, as compared with the earlier computed angle of about 21^{o}.

The correct values should probably lie between those found by the two methods. The calculated values of 7.9 and 8.11 for movement of the j and k planes, and the angle of 21^{o} relative to the apex, are too high because of neglect of the effect of movement of the j and k planes on observed values of φ_g. The velocity components of 2.18 and 1.65 km/sec, and the angle of about $1/2^{o}$, found with the computer run, tended to be too low because it was necessary to neglect the directions from which the greatest components of velocity in the j and k directions would come, but tended to be too high because no correction was made for changes in the values of φ_g.

The effect of the movement of the planes on the values of φ_g could readily be calculated in a later analysis. The frequency determined in the present analysis for a meteor having a given heliocentric velocity vector would simply be multiplied by the ratio of its velocity relative to the moving origin of the i, j, and k planes to the geocentric velocity.

For an ideal analysis it would be desirable to have a repetition of the work reported in reference 7 at three additional locations of the cameras: (1) within the arctic circle, (2) within the south temperate zone, and (3) within the antarctic circle. The data from the additional positions on the Earth's surface would provide coverage of the entire 4π steradians of solid angle surrounding the Earth, except a small solid angle centered exactly in the direction of the Sun. Considering the foregoing discussion, it should not be surprising if such an ideal analysis with the additional data available would show exactly equal flux of kinetic energy across any plane with origin moving at an angle of only a few degrees to the apex of Earth movement.

With the demonstrated existence of such a condition in Earth orbit about the Sun, a similar condition could reasonably be expected elsewhere within the solar system, also. The sample of reference 7, with similar samples from the other three suggested regions, would provide samples for a family of heliocentric vector velocities coming from any location within the solar system. The corresponding velocities and directions at such locations are easily computed. As a bimodal log-normal equation has been shown to fit the distribution of any velocity component satisfactorily in Earth's orbit, such an equation might reasonably be assumed to apply elsewhere also. The maximum possible velocity and a minimum possible velocity (to avoid passage into the Sun's atmosphere) can be computed for any direction of motion at any position within the solar system.

All the known parameters and conditions described would seem to be sufficient to construct a reasonable tentative distribution of velocity and mass and a flux rate for all locations. A check would have to be made, of course, as to whether the meteor sample included enough asteroidal meteors to indicate that the same findings applied to them.

DISCUSSION OF RESULTS

All the work reported here and in references 1 to 5 has culminated in the velocity histograms shown in figures 1 to 3; equation (3) with the values of constants shown in table I governing distribution of normal components of impact velocity; the concentration factors shown in table II; the values of $\overline{v^n_{norm}}$ shown in figures 4 to 6; and the armor thicknesses shown in table III. The preliminary work reported in references 1 to 5 seems to provide a firm foundation for those results.

The computational results in table III show a marked advantage of a particular orientation only in the case of the trailing side of the i oriented plane. The advantage in that case, however, is substantial and can readily be used.

For example, a vulnerable area of 2000 square feet (185.8 m^2) may be assumed, composed of two parallel plane sheets of armor. Then, if the sheets have the i orientation with a 99.5-percent probability of no destructive impact for each sheet (a 99 percent probability for the combination) the combined thickness for leading and trailing sheets, as shown in table III would be 0.808 centimeter (0.318 in.) an average of 0.408 centimeter (0.159 in.). With the j or k orientation, having symmetrical meteoroid influx, the combined thickness would be 1.18 centimeter (0.464 in.) or 1.00 centimeter (0.394 in.), that is, 46 percent or 24 percent greater than with the i orientation.

If the vulnerable area of 2000 square feet (185.8 m^2) is assumed to be entirely in the form of cylinders of uniform wall thickness, with no consideration for shadowing of one surface by another, then the necessary thicknesses for the i, j, and k orientations are 0.547, 0.481, and 0.521 centimeter (0.215, 0.190, and 0.205 in.). It is seen that the i orientation requires 13 percent and the k orientation 8 percent greater thickness than the j orientation.

If cylinders of nonuniform wall thickness are assumed, an approximation of the necessary thickness at four points on the cylinder cross section may be obtained by use of the results for planes in table III. Those four points are the points of tangency of the cylindrical cross section with four planes having i, j, or k orientation as the case may be. Thus, an i tube would have two j oriented and two k oriented tangent plane surfaces as illustrated in sketch (b). There would be approximately an area of 1000 square feet (92.9 m^2) in each orientation, with a 99.5 percent probability of no destructive impact for each (a combined probability of 99 percent). From the tabulated results in table III, the average wall thickness would then be 0.545 centimeter (0.2145 in.), with 0.50 centimeter required for the tangent k planes and 0.59 for the tangent j planes. Similar treatment for a j or k oriented tube would involve 500 square feet (46.5 m^2) and a 99.75 percent probability for each of the i planes (leading and trailing) with 1000 square feet (92.9 m^2) and 99.5 percent probability for the symmetrical k or j planes. The consequent average thicknesses for the j and k oriented tubes would

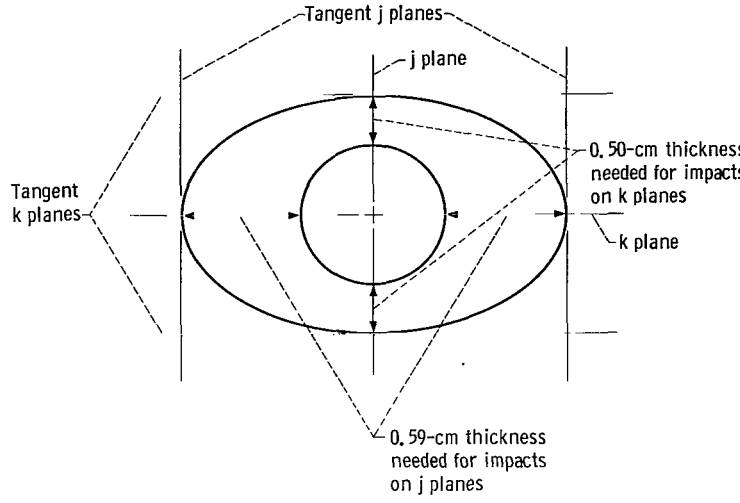

Cross section of i oriented cylinder with exaggerated variation of wall thickness

(b)

be 0.452 and 0.497 centimeter (0.178 and 0.196 in.). These results indicate an advantage of 20.5 and 10 percent for the j orientation as compared with the i or k and an advantage of about 7 percent for the j oriented tube of variable thickness over the j oriented tube of uniform thickness.

A further advantage could be obtained by suitable orientation of panels of tubes. With use of the most favorable j orientation of tubes of nonuniform wall thickness, a large number of such tubes could be placed side by side with all their centerlines lying within a single plane, whether i oriented or k oriented. With i orientation of the plane of the panel, as shown in sketch (c) below, tubes would, at least to some extent,

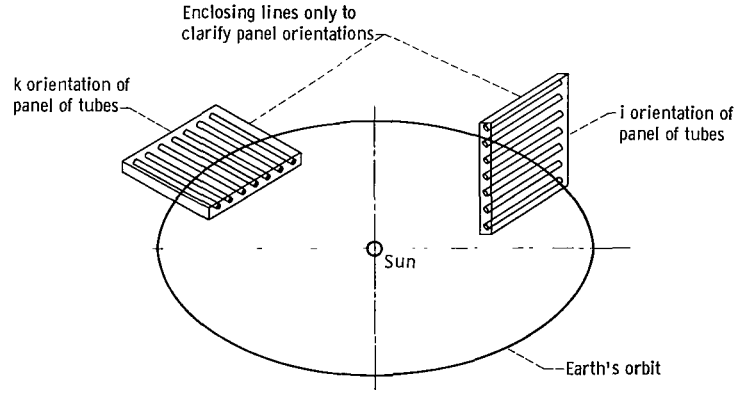

(c)

TABLE IV. - DATA USED IN CONSTRUCTION OF HISTOGRAMS FOR NORMAL COMPONENT OF IMPACT VELOCITY ON PLANES, CYLINDERS, AND SPHERES

Velocity, km/sec (I)	Percentage of all sporadic meteors with impact velocity between I and I + 1								
	Full velocity on spherical or randomly oriented plane surface	Normal component only							
		Plane surface whose normal always points in direction stated				Cylindrical surface whose axis always points in direction stated			Spherical surface
		Direction of movement of Earth in its orbit		Toward Sun	Perpendicular to ecliptic plane	Direction of movement of Earth in its orbit	Toward Sun	Perpendicular to ecliptic plane	
		Leading side	Trailing side						
0	0	6.5732	1.5325	0.2150	1.5865	1.0611	1.6925	1.3149	1.2706
1	.2704	8.1473	3.8174	1.1860	4.6238	3.1646	4.9682	3.5136	3.6291
2	1.0296	13.4415	5.9704	1.9630	5.7138	4.3097	7.0795	5.2125	5.2710
3	.5130	17.2790	8.1371	5.6162	4.8475	5.6099	9.0543	7.4423	6.8022
4	2.9600	7.5926	17.1491	4.8446	8.7479	7.2160	10.9618	7.5733	7.7142
5	2.0318	7.0298	12.5949	6.6070	11.5907	6.7885	11.4111	7.7189	8.2930
6	2.7082	13.6890	16.4395	5.0747	8.9228	7.3753	10.9419	8.5386	9.0178
7	9.0513	4.1735	18.1031	8.3602	8.4837	7.4244	9.7357	8.2444	8.6125
8	6.2843	1.9316	10.6094	7.8416	5.1294	7.5947	7.0078	8.7261	7.6138
9	6.5774	1.1193	4.3381	7.1637	8.1732	7.1482	5.7238	6.5540	7.0513
10	7.0204	1.7880	.2665	5.0596	4.6995	5.7444	4.3772	5.8750	6.3905
11	9.4131	1.9782	.9409	8.2002	5.1469	6.0317	3.8775	5.3161	5.2535
12	7.7647	.9120	.0260	3.6104	3.7602	5.2222	2.5981	3.9572	4.3015
13	7.1902	.8027	0	5.7946	5.0821	3.9251	2.1453	3.2478	3.4277
14	6.4739	1.4562	↓	2.3588	1.6657	3.1523	1.6217	2.6220	2.6823
15	4.1989	2.6201	↓	2.2329	1.4469	2.5991	.9933	1.9926	2.1309
16	3.6807	.4536	↓	3.8782	.5819	2.2138	.6993	1.9178	1.7558
17	3.1782	1.2977	↓	2.2415	1.2330	2.0230	.7820	1.5263	1.4960
18	3.1263	1.1581	.0054	3.0806	1.2587	1.8489	.5485	1.4625	1.2256
19	2.3844	.7511	0	2.2110	.7287	1.5393	.4436	1.1954	1.0076
20	1.8870	.4091	↓	2.1668	.6004	1.3573	.4071	.9025	.8334
21	1.8402	.2850	↓	.9519	.8871	1.0530	.3697	.6816	.6733
22	1.4215	.4104	↓	.9631	.9675	.9019	.3890	.6475	.5754
23	1.0350	.0525	↓	1.5230	.6456	.8333	.2595	.6483	.4832
24	1.3859	.1130	↓	1.5475	.6217	.7982	.2337	.5631	.3978
25	1.1487	.1198	↓	.9606	.2853	.5262	.1521	.3980	.3115
26	.7544	.1154	↓	1.0116	.2432	.4484	.1423	.3610	.2514
27	.9123	.0471	↓	.8020	.2475	.3650	.1392	.2803	.2060
28	.3758	.0981	.0565	.3746	.2670	.2967	.1305	.2049	.1626
29	.3497	.3090	0	.5786	.3673	.2655	.1204	.1626	.1433

30	.3225	.0210		.2454	.0470	.1814	.0619	.1390	.1244
31	.3623	.0686		.2565	.2435	.1724	.0695	.1204	.1076
32	.1415	.1092		.3605	.0883	.1524	.0573	.1220	.0933
33	.2310	.0656		.1564	.1991	.1344	.0586	.1268	.0852
34	.3015	.0316		.1786	.1347	.1080	.0611	.0918	.0722
35	.1901	.0344		.1152	.1640	.0885	.0558	.0742	.0598
36	.1129	.1442	.0025	.0532	.1514	.0792	.0517	.0570	.0522
37	.1559	.1189	0	.0356	.1676	.0726	.0439	.0544	.0471
38	.1635	.0576		.0676	.0584	.0577	.0351	.0487	.0401
39	.1198	.0820		.0386	.0330	.0395	.0390	.0370	.0343
40	.1261	.0680		.0116	.0745	.0269	.0301	.0314	.0298
41	.0508	.1130		.0353	.0319	.0205	.0260	.0275	.0251
42	.0720	.1257		.0049	.0284	.0070	.0252	.0226	.0223
43	.0767	.0957		.0020	.0114	.0049	.0280	.0179	.0197
44	.0605	.2153	.0107	.0079	.0024	.0034	.0250	.0161	.0165
45	.0530	.1879	0	0	0	.0030	.0241	.0121	.0147
46	.0341	.0865		0	.0031	.0016	.0201	.0107	.0133
47	.0193	.0261		.0007	0	.0018	.0167	.0114	.0124
48	.0059	.1644		.0036	.0037	.0011	.0180	.0131	.0122
49	.0281	.1750		0	0	.0017	.0200	.0136	.0118
50	.0037	.2144				.0015	.0155	.0163	.0114
51	.0151	.1655				.0005	.0163	.0166	.0111
52	.0193	.0564				.0002	.0201	.0107	.0108
53	.0227	.1253				.0002	.0185	.0118	.0101
54	.0207	.0881		.0029		.0003	.0175	.0108	.0095
55	.0138	.0505		.0036		.0004	.0183	.0102	.0091
56	.0230	.0942		0		.0006	.0157	.0098	.0087
57	.0186	.1249				.0003	.0144	.0078	.0081
58	.0327	.1124				.0003	.0128	.0083	.0072
59	.0167	.0754			.0019	.0001	.0119	.0052	.0065
60	.0406	.0120			0	.0001	.0108	.0046	.0056
61	.0272	.1124				.0001	.0086	.0053	.0046
62	.0216	.0929				.0002	.0085	.0063	.0040
63	.0326	.0436				0	.0075	.0041	.0031
64	.0189	.1091					.0055	.0046	.0023
65	.0056	.0503					.0046	.0032	.0020
66	.0120	.0478					.0052	.0035	.0018
67	.0117	.0505					.0032	.0029	.0014
68	.0090	.0292					.0024	.0031	.0012
69	.0118	.0525					.0021	.0018	.0010
70	.0085	.0500					.0024	.0011	.0006
71	.0067	.0159					.0017	.0008	.0004
72	.0068	0					.0010	.0008	.0003
73	0	.0402					.0006	.0006	.0001
74	0	0					.0003	.0002	.0002
75	.0018	0					.0003	.0003	.0001
76	.0016	.0207					.0006	.0005	.0001
77	.0025	.0216					.0001	.0001	0
78	0	0					0	0	0
79	0	0					0	0	0

shield each other on the sides tangent with the k plane. (Lines enclosing panels of tubes in the sketch (c) are intended only to clarify panel orientation.) With the panel of tubes lying in the k plane (also shown in the sketch), the tubes would shield each other on the sides tangent to the i plane. As the two unshielded k planes require 24 percent greater armor thickness than the average of the two i planes, obviously the shielding of the k oriented surfaces by the i orientation of the panel of tubes is more desirable than the shielding of the i oriented surfaces by the k orientation of the panel.

If a damage criterion is used that includes as factors v_{norm}^{ϵ} and m^{λ} with ϵ smaller than in equation (4), with λ larger, or both, the value 3.332 for the exponent of v_{norm} in equation (6) is reduced accordingly. The effects of orientation are consequently considerably altered. Obviously a lower value of the exponent requires thinner armor than a higher value. But, in the function $\overline{v_{norm}^{n}}$, the higher values of n place greater weight on the highest values of v_{norm}. Thus, with n approaching infinity the value of the function $\left(\overline{v_{norm}^{n}}\right)^{1/n}$ approaches the highest value of v_{norm} for any meteor. With n = 1, all weighting in favor of higher values of v_{norm} is gone and we have a simple arithmetic average. As n approaches zero, we approach a geometric average which is weighted somewhat in favor of lower values of v_{norm}.

From inspection of figure 4, the advantage of the trailing side of the i oriented plane is progressively lost with diminishing n until, with values of n less than about 2.0, it becomes even worse than the leading side of that plane. The leading side of the i plane becomes no worse than either side of the j plane when n is about 3.8, and it becomes as good as the k plane with n of about 3.0. From figure 5 the differences in effect of the i, j, and k orientations for a tube of uniform thickness are increased as n is reduced from the value 3.332. As n is increased, orientation loses effect when n is about 4.25. With higher values yet, the differences of effect of the three orientations reverse, so that the i orientation becomes best.

An intuitive check on consistency of results has been made by determining that the computational result for critical thickness of a sphere as shown in table III is, within 1 percent, the same as the average for planes and within $2\frac{1}{2}$ percent the same as the average for cylinders with the three principal orientations. A more definite check on the result for a sphere is the fact that it is, within 2 percent, the same as determined with use of a different method in reference 4. In that case, a histogram was constructed with use of the data shown in column 2 of table IV, for gross impact velocities. An equation of the same form as equation (3) was fitted to that histogram and that equation was integrated to provide values of $\overline{v^{n}}$. Then, with φ_g equal to unity, and with use of an expression for $\overline{v_{norm}^{n}}$ in terms of $\overline{v^{n}}$, the value of t_{cr} was determined with an equation equivalent to (6).

The analysis here has dealt entirely with conditions far enough from Earth that Earth's gravity has negligible effect on meteoroid velocity. The condition at the upper

limit of Earth's atmosphere was also treated, for a sphere, in reference 4. The necessary armor thickness for the sphere near Earth proved to be about 19 percent greater than far from Earth.

The results for the near-Earth condition for a sphere were simply derived in reference 4 from the far-from-Earth results. But the treatment of effects of orientation of planes and cylinders for near-Earth conditions would be much more complex and could not be included in the present analysis. The author believes that the relative advantages of particular orientations would remain of the same nature as for far-from-Earth conditions, but that they would be slightly reduced. This opinion is based on the fact that substantial changes of direction of motion of meteoroids by Earth's gravitation exists only when values of v_G are too small for a meteoroid to represent a substantial part of the total hazard.

Although the results of this study are directly applicable only to space missions in or near Earth's orbit about the Sun, it is believed the results can be extended by the methods outlined to deduce a valuable tentative model at substantial distances from that orbit.

Lewis Research Center,
National Aeronautics and Space Administration,
Cleveland, Ohio, June 22, 1970,
131-05.

APPENDIX A

SYMBOLS

A	vulnerable area exposed to meteoroid hazard, m^2
A_{eff}	projection of vulnerable area exposed to meteoroid hazard upon a plane normal to meteoroid path, unspecified units
a	semi-major axis of elliptical orbit of meteoroid, or constant as used in standard eq. (2) for hyperbolic orbit, AU
b	semi-minor axis of elliptical orbit of meteoroid, or constant as used in standard eq. (2) for hyperbolic orbit, AU
C_i	constant in eq. (3), dimensionless
c	an orbital element for an elliptical, parabolic, or hyperbolic orbit, as illustrated in fig. 7(a), AU
$E_{e(s)}$	energy of escape from Sun at positions in Earth's orbit, ft-lb (1.356 J)
$E_{k(E)}$	kinetic energy associated with orbital motion of a mass corresponding to one unit weight in Earth's orbit, ft-lb (1.356 J)
e	eccentricity of conic section (orbit of meteoroid), dimensionless
$F_{gs(\rho)}$	gravitational force exerted by Sun on mass corresponding to unit weight on Earth's surface, but at distance ρ from Sun, lb (4.448 N)
$F(Z_R)_{av}$	a statistical function developed in reference 1 involving zenith angle of meteor, its position within camera field of view, and azimuth of its path, and their effects on density of photographic trace, unspecified units
$f(\ )$	(with any argument within parentheses) statistical frequency of occurrence of given value of argument (for v_{norm}, approximately fraction of all impacts for which v_{norm} has given value ± 0.5 km/sec)
g	acceleration due to Earth's gravity at Earth's surface, ft sec^{-2} (0.3048 m sec^{-2})
i	direction of the apex of Earth's movement, also inclination of orbit of meteoroid to ecliptic plane as used in ref. 7 (equal to γ or supplement of γ as used here), deg
$\vec{i}$	unit velocity vector in the i direction, km/sec

i_{cyl} for meteoroid that passes through axis of i, j, or k oriented cylinder, angle of incidence of meteoroid's path relative to axis of cylinder, deg

i_{pl} angle of incidence of meteor path relative to plane with i, j, or k orientation, deg

j direction within ecliptic plane and approximately away from Sun but exactly perpendicular to apex of Earth motion

$\vec{j}$ unit velocity vector in j direction, km/sec

k direction perpendicular to ecliptic plane, southward

$\vec{k}$ unit velocity vector in k direction, km/sec

m mass of meteoroid, g

p average number of destructive impacts by meteoroids per mission or semi-latus rectum of meteor orbit, AU

p_E sec per year

q perihelion distance of meteoroid orbit, AU

q' aphelion distance of meteoroid orbit, AU

r_{cyl} radius of i, j, or k oriented cylinder, unspecified units

r_E radius of Earth's orbit, ft or AU

r_{sph} radius of sphere, unspecified units

S_{cyl} cylindrical surface area for an i, j, or k oriented cylinder, unspecified units

S_{sph} surface area of sphere, unspecified units

T duration of space mission, sec

t_{cr} critical value of thickness of armor necessary to provide a given probability of no destructive impact by a meteoroid, cm

v_E velocity of Earth in its orbit, km/sec, except where shown as ft/sec

$v_{e(s)}$ velocity of escape from Sun at positions in Earth's orbit, km/sec except where shown as ft/sec

v_G scalar value of velocity of meteoroid relative to moving Earth, corrected for acceleration by Earth gravity, as given in ref. 7, km/sec

$\vec{v_G}$ vector velocity of meteoroid relative to moving Earth, corrected for acceleration by Earth's gravity, km/sec

v_H scalar value of velocity of meteoric particle relative to Sun, corrected for acceleration by Earth's gravity, as given in ref. 7, km/sec

$\vec{v_H}$ vector velocity of meteoroid relative to Sun with scalar value v_H, km/sec

$\vec{v_I}$ component of the vector velocity of a meteoroid $\vec{v_G}$ having scalar value I and normal to surface of cylinder with i, j, or k orientation, km/sec

$\vec{v}$ (with subscripts i, j, or k) component of vector $\vec{v_H}$ in i, j, or k direction, km/sec

$\vec{v}$ (with subscripts ir, jr, or kr) component in i, j, or k direction of vector velocity of meteoroid relative to moving Earth $\vec{v_G}$, km/sec

$\vec{v}$ (with subscripts ij, jk, or ki) component lying entirely within k, i, or j oriented plane, respectively, of vector velocity of meteoroid relative to moving Earth $\vec{v_G}$, km/sec

$\vec{v_i'}$ component of $\vec{v_H}$ in i direction under the usually false assumption that meteoroid orbit is within ecliptic plane, km/sec

v_{norm} scalar value of component of impact velocity of a meteoroid normal to impacted surface, km/sec

v_∞ scalar velocity of meteoric particle relative to Earth's atmosphere before deceleration by atmosphere, km/sec

x one of rectangular coordinates in standard equations for conic sections, AU

y one of rectangular coordinates in standard equations for conic sections, AU

Z_R angle of meteor path through atmosphere relative to zenith, deg

α right ascension of true radiant of meteor (ref. 7), deg

γ inclination of orbit of meteoroid to ecliptic plane (arbitrarily measured with value equal to or less than 90), deg

δ declination of true radiant of meteor (see ref. 7), deg

δ_I value of angle at which normal component of impact velocity of a particular meteoroid upon an i, j, or k oriented cylinder or upon surface of a sphere is equal to I, deg

δ_i offset of mode in i^{th} term of log-normal distribution eq. (3), km/sec

ϵ exponent of v_{norm} in damage criterion

ϵ_t percent elongation of armor material

θ angle between apex of Earth motion and line within ecliptic plane that is perpendicular to major axis of orbit of meteoroid under usually incorrect assumption that meteoroid's orbit is within ecliptic plane (see fig. 7(a)), deg

λ exponent of m in damage criterion or angle between vector velocity of meteoroid $\vec{v}_H$ and apex of Earth motion, under usually incorrect assumption that meteoroid orbit is within ecliptic plane, deg

λ_{cyl} length of an i, j, or k oriented cylinder, unspecified units

μ_i logarithmic modal value in term of distribution eq. (3), natural logarithm of velocity in km/sec

ρ distance from Sun, ft (m)

ρ_p density of particle impacting upon armor, g/cm^3

ρ_t density of armor material, g/cm^3

σ_i logarithmic standard deviation in a term of distribution eq. (3), natural logarithm of value of velocity in km/sec

φ angle between vector velocity of meteoroid $\vec{v}_H$ and line within ecliptic plane that is perpendicular to major axis of orbit of meteoroid under usually false assumption that meteoroid's orbit is within ecliptic plane (see fig. 7(a)), deg

$\varphi_{cyl(\ )I}$ (with i, j, or k within parentheses and with integral value of I) $\varphi_{cyl(i)}$, $\varphi_{cyl(j)}$, or $\varphi_{cyl(k)}$ times fraction of cases in which given meteoroid should be expected to strike cylinder with i, j, or k orientation with normal component of impact velocity between I and I + 1 km/sec

$$\left(\sum_{n=0}^{79} \varphi_{cyl(m)n} = \varphi_{cyl(m)} \text{ with significance of m as i, j, or k}\right)$$

φ_g concentration factor, frequency of meteoroid impacts upon structure under specified condition relative to frequency of impacts upon same structure randomly oriented

φ'_g summation of values of $\varphi_{m(n)}$ for particular significance of m and particular significance of n

$\varphi_{g(qu)}$ same as φ_g, but applying only to meteoroids for which $\vec{v}_j \cdot \vec{j}$ was negative and $\vec{v}_k \cdot \vec{k}$ was positive

φ_I fraction of $\varphi_{cyl(i)}$, $\varphi_{cyl(j)}$, or $\varphi_{cyl(k)}$ for which normal component of impact velocity of meteoroid upon cylinder is between I and I + 1 or fraction of φ_w for which normal component of impact velocity on sphere is between I and I + 1

$\varphi_{m(n)}$ (m signifying pl or cyl and n signifying i, j, or k) a modification of the weighting factor φ_w for use with a particular meteor, for a plane or cylinder with i, j, or k orientation, to take into account reduced effective vulnerable area because angle of incidence is not the most unfavorable.

$\varphi_{m(r)}$ (m signifying cyl or pl) same as φ_w but referred to randomly oriented cylinder or plane

φ_{or} probability of impact of given meteoroid upon given structure (plane or cylinder), with i, j, or k orientation, divided by probability of impact upon same structure with basic (worst) orientation relative to meteoroid path

$\varphi_{or(av)}$ average value of φ_{or} for given structure with given orientation

φ_s weighting factor for correction of spacewise bias in photography of meteors inverse value of which was developed and computed in work reported in ref. 5

$\varphi_{sph(I)}$ that part of φ_w applying to impact upon sphere with normal component of impact velocity between I and I + 1 km/sec

φ_w weighting factor developed in refs. 1 to 5, to provide simultaneous correction for mass, velocity, and spacewise biases in photography of meteors

$\varphi_{w(r)}$ same as φ_w but referred to randomly oriented area rather than area always normal to meteoroid path

APPENDIX B

DATA USED FOR EACH METEOR

Redundancy exists in the orbital parameters of meteors given in reference 7. Some of those parameters are (1) the angle δ of the true radiant, (2) the angle α of the true radiant, (3) the velocity of the meteoroid relative to the Sun, v_H, corrected for the acceleration by Earth gravitation, (4) the semi-major axis a, (5) the eccentricity e, (6) the perihelion distance q, (7) the aphelion distance q', and (8) the inclination of the meteoroid's orbit to the ecliptic plane γ (designated i in ref. 7).

Because of symmetry assumed in this analysis, unnecessary and useless complications would be involved in making use of the values of δ and α, or any of several other parameters given in reference 7 and not listed here. Of the parameters listed, three only are needed, including the orbital inclination γ. Values of a, q, and γ were used in determination of angles defining the direction of movement of the meteoric particle relative to the Earth's orbital plane and the apex of the Earth's movement within that plane. The value of v_H as given in reference 7 was used directly as the velocity of the particle.

Arrangements were made within the computer program to use the values of a and q to compute the eccentricity e, the velocity v_H, and the aphelion q'. These values were computed by well known methods that will not be described here and were compared for all meteors used with the values given in reference 7. No substantial disagreements were found.

APPENDIX C

BASIC CONSTANTS USED IN RESOLUTION OF VELOCITIES OF METEORS

Certain basic constants will be explained here, which were needed in the process of solving for velocity components, beginning with given orbital parameters. For convenience, the customary U.S. system of units was used in this appendix and the results to be used in the analysis were converted to SI units after the determinations were completed. The obvious constants will not be derived.

The radius of Earth's orbit was taken as

$$r_E = 4.9106 \times 10^{11} \text{ ft } (14.9714 \text{ km}) \tag{C1}$$

The length of year was taken as

$$p_E = 3.1558 \times 10^{7} \text{ sec } (365.256 \text{ days}) \tag{C2}$$

The Earth orbital velocity was taken as

$$v_E = \frac{2\pi r_E}{p_E} = 9.7770 \times 10^{4} \text{ ft/sec } (32.069 \text{ km/sec}) \tag{C3}$$

The acceleration due to Earth's gravity at surface, at the camera sites in New Mexico, was

$$g = 32.2 \text{ ft/sec}^2 \ (9.815 \text{ m/sec}^2) \tag{C4}$$

The kinetic energy of a mass corresponding to one unit weight in Earth's orbit is

$$E_{k(E)} = \frac{1}{2g} v_E^2 = 1.4843 \times 10^{8} \text{ ft-lb } (2.011 \times 10^{8} \text{ J}) \tag{C5}$$

The velocity of escape from the Sun at a position in Earth's orbit was taken as

$$v_{e(s)} = \sqrt{2}\, v_E = 1.3827 \times 10^{5} \text{ ft/sec } (42.14 \text{ km/sec}) \tag{C6}$$

Equation (C6) is derived by integrating the Sun's gravitational force from a distance of one astronomical unit to infinity. The escape kinetic energy must be

$$E_{e(s)} = \int_{r_E}^{\infty} F_{gs(\rho)}\, d\rho \tag{C7}$$

where $F_{gs(\rho)}$ is the force exerted by the Sun on a mass corresponding to one unit weight at any distance ρ. An expression for $F_{gs(\rho)}$ may be derived from the equality of centrifugal force and gravitational force of a particle moving in the Earth's orbit as follows:

$$F_{gs(r_E)} = \frac{1}{g}\frac{v_E^2}{r_E} \tag{C8}$$

and as the Sun's attraction varies inversely as the square of the distance,

$$F_{gs(\rho)} = \frac{1}{g}\frac{v_E^2}{r_E}\left(\frac{r_E}{\rho}\right)^2 \tag{C9}$$

From equations (C7) and (C9),

$$E_{e(s)} = \frac{1}{g} v_E^2 r_E \int_{r_E}^{\infty} \rho^{-2}\, d\rho = \frac{1}{g} v_E^2 \tag{C10}$$

On comparison of equations (C5) and (C10) we see that $E_{e(s)}$ is twice $E_{k(E)}$. So equation (C6) follows because velocities must vary as the square roots of kinetic energy.

APPENDIX D

THREE ORTHOGONAL COMPONENTS OF METEOROID VELOCITY RELATIVE TO EARTH

Figure 7 illustrates the method of resolution of the heliocentric velocity of a meteoroid v_H into three orthogonal components. As an intermediate step, the orbit of the particle was treated as being within the plane of the ecliptic (fig. 7(a)). Although two points of intersection always exist, only one need be considered because of symmetry in the use that is to be made of the results. The upper intersection in figure 7(a) was chosen for consideration.

Also because of symmetry, no discrimination was necessary between positive and negative j and k directions. In figure 7(a), for convenience, the j direction was taken as the reverse of the actual for the meteors in direct orbits that were treated. Moreover, at this stage of the analysis, all meteors were treated as having direct motion, that is, angular velocity about the Sun in the same sense as for Earth. Discrimination between direct and retrograde movement in the orbit was left till later.

The heliocentric vector velocity of a meteoroid will be designated as $\overrightarrow{v_H}$. Then, of course,

$$v_H = |\overrightarrow{v_H}| \tag{D1}$$

In the intermediate step, this vector velocity $\overrightarrow{v_H}$ was resolved into two components $\overrightarrow{v_j}$ and $\overrightarrow{v_i'}$. The component $\overrightarrow{v_j}$ was the final component wanted in the j direction, but the component $\overrightarrow{v_i'}$ was simply the vector velocity $\overrightarrow{v_H}$ minus $\overrightarrow{v_j}$. It was the component velocity in the i direction that would have existed if the particle's orbit had actually been in the ecliptic plane as shown in figure 7(a).

Obviously, in the intermediate step,

$$\overrightarrow{v_j} = v_H \sin \lambda \vec{j} \tag{D2}$$

and

$$\overrightarrow{v_i'} = v_H \cos \lambda \vec{i} \tag{D3}$$

where $\vec{i}$ and $\vec{j}$ are unit vectors in the i and j directions, and λ is the angle be-

tween the tangents to the meteoroid path and Earth's path in their orbits at the time of impact (fig. 7(a)).

Methods used for finding the value of the angle λ will now be described for elliptical, parabolic, and hyperbolic orbits. Sources of various equations will not be stated in cases where they are well known and are obtainable in most textbooks on analytic geometry.

Elliptical Orbits - Angle Between Paths of Meteoroid and Earth

If c represents distance from the center of an elliptical orbit to the applicable focus shown in figure 7(a), then, obviously,

$$c = a - q \tag{D4}$$

Then the semi-minor axis of the orbit is

$$b = \sqrt{a^2 - c^2} \tag{D5}$$

and the eccentricity is

$$e = \frac{c}{a} \tag{D6}$$

Now the angle θ with vertex at the Sun in figure 7(a) may be found with use of the standard polar equation of an ellipse about its right-hand focus as a center,

$$r_E = \frac{p}{1 + e \cos \theta} \tag{D7}$$

and the equation for the semi-latus rectum

$$p = \frac{b^2}{a} \tag{D8}$$

(r_E is unity in eq. (D7) and elsewhere with distances expressed in astronomical units). By combining equations (D7) and (D8) and rearranging,

$$\cos \theta = \frac{b^2 - r_E a}{r_E ae} \tag{D9}$$

Next, the slope of the tangent to the particle orbit at the point of intersection of the orbits was determined. By implicit differentiation of the equation of the ellipse

$$\frac{x^2}{a^2} + \frac{y^2}{b^2} = 1 \tag{D10}$$

the slope is found as

$$\frac{dy}{dx} = -\frac{b^2 x}{a^2 y} \tag{D11}$$

or

$$\frac{dy}{dx} = -\frac{b^2(c + r_E \cos \theta)}{a^2 r_E \sin \theta} \tag{D12}$$

The angle φ as shown in figure 7(a), then, is

$$\varphi = \tan^{-1}\left(\frac{dy}{dx}\right) - \frac{\pi}{2} \tag{D13}$$

At this point, the angle λ (fig. 7(a)) is determined as

$$\lambda = \theta - \varphi \tag{D14}$$

Parabolic Orbits - Angle Between Paths of Meteoroid and Earth

The equation for a leftward extending parabola like that shown in figure 7(a) is

$$y^2 = 4cx \tag{D15}$$

in which c must be negative. As may be seen from figure 7(a),

$$r_E^2 = (c - x)^2 + y^2 \tag{D16}$$

From equations (D15) and (D16)

$$r_E^2 = c^2 - 2cx + x^2 + 4cx \tag{D17}$$

or

$$-r_E = c + x \tag{D18}$$

and

$$x = -r_E - c \tag{D19}$$

As, for the parabola,

$$c = -q \tag{D20}$$

an expression for θ may be written by reference to the figure,

$$\cos \theta = \frac{q + x}{r_E} \tag{D21}$$

or, from equations (D19), (D20), and (D21),

$$\cos \theta = \frac{2q}{r_E} - 1 \tag{D22}$$

The angles θ and λ may now be found as follows: From equations (D15), (D19), and (D20),

$$y^2 = -4q(-r_E + q) \tag{D23}$$

or

$$y = 2\sqrt{qr_E - q^2} \tag{D24}$$

By implicit differentiation of equation (D15), with substitution according to equation (D20),

$$\frac{dy}{dx} = -\frac{2q}{y} \tag{D25}$$

From equations (D24) and (D25),

$$\frac{dy}{dx} = -\sqrt{\frac{q}{r_E - q}} \tag{D26}$$

The angles φ and λ may now be found with equations (D13) and (D14) as before.

Hyperbolic Orbits - Angle Between Paths of Meteoroid and Earth

Equation (2) was used for the hyperbolic orbits. The variable a as used in the denominator in the first term of the equation was made equal to the absolute value of a as given in reference 7. For the leftward branch of the hyperbola as shown in figure 7(a), the value of x determinable with equation (2) is always negative.

As shown in figure 7(a), for the hyperbola,

$$c = q + a \tag{D27}$$

Hence, with the well known relation,

$$c = \sqrt{a^2 + b^2} \tag{D28}$$

the value of b may be expressed as

$$b = \sqrt{(2a + q)q} \tag{D29}$$

With use of the polar equation for the leftward branch of a hyperbola about the leftward focus, the condition in figure 7(a),

$$r_E = \frac{p}{1 + e \cos \theta} \tag{D30}$$

In equation (D30) e and p are expressed by equations (D6) and (D8) for the hyperbola as they were for the ellipse. Then, from equations (D6), (D8), and (D30),

$$\cos \theta = \frac{b^2 - r_E a}{r_E c} \tag{D31}$$

By implicit differentiation of equation (2),

$$\frac{dy}{dx} = \frac{b^2 x}{a^2 y} \tag{D32}$$

By inspection of figure 7(a),

$$x = -c + r_E \cos \theta \tag{D33}$$

and

$$y = r_E \sin \theta \tag{D34}$$

From equations (D32) to (D34),

$$\frac{dy}{dx} = \frac{b^2(r_E \cos \theta - c)}{a^2 r_E \sin \theta} \tag{D35}$$

After determination of dy/dx with equations (D32) to (D34), the angles φ and λ may be found with use of equations (D13) and (D14), as with the elliptical and parabolic orbits.

Parts of Heliocentric Velocity Resolution Common to All Orbital Types

Because of the simplifying approximation of Earth's orbit as a circle, application

of orbital equations was not possible for meteors having a value of q greater than 1 astronomical unit or values of q' less than such a value. For all such meteors, the value of q or q' was taken as unity, and impact with Earth's atmosphere was assumed to have occurred exactly at the point of tangency of the orbits of the particle and the Earth, under the presumption used in this intermediate step that the orbit of the meteoroid lay entirely within the ecliptic plane. Hence, for such cases, as well as for cases in which the value of q or q' was given in reference 7 as exactly 1.00, no discrimination was needed in accordance with the preceding sections between elliptic, parabolic, and hyperbolic orbits. Instead of equations (D2) and (D3), the following were used

$$\vec{v_i'} = v_H \vec{i} \tag{D36}$$

and

$$\vec{v_j} = 0 \tag{D37}$$

After determination of the values of $\vec{v_i'}$ and $\vec{v_j}$ with use of equations (D2) and (D3) or equations (D36) and (D37), the second and final stage in determining the three principal components of $\vec{v_H}$ was performed as illustrated in figure 7(b). The relation of this view to figure 7(a) is shown in figure 7(a); that is, figure 7(b) shows the orbits as they would be seen by a viewer looking in the direction from Sun to Earth. In figure 7(b), however, the orbit of the meteor particle has been rotated about the line that extends from Sun to Earth through the angle γ. This angle is the same as i, given in reference 7, except that when the particle was in retrograde motion and the value of i was consequently shown as greater than 90^o, the angle γ was made equal to the supplement of i.

As is obvious by inspection of figure 7(b),

$$\vec{v_k} = |\vec{v_i'}| \sin \gamma \vec{k} \tag{D38}$$

where $\vec{k}$ is a unit vector in the k direction (normal to both $\vec{i}$ and $\vec{j}$ introduced earlier), and

$$\vec{v_i} = |\vec{v_i'}| \cos \gamma \vec{i} \tag{D39}$$

From equations (D3) and (D38),

$$\vec{v_k} = v_H \cos \lambda \sin \gamma \vec{k} \tag{D40}$$

and from equations (D3) and (D39),

$$\vec{v_i} = v_H \cos \lambda \cos \gamma \vec{i} \tag{D41}$$

Equation (D2) or (D37) and equations (D40) and (D41) provide the desired three principal components of the velocity $\vec{v_H}$ for particles in direct motion. Equations (D2), (D37), and (D40) are also valid for particles in retrograde motion because of symmetry. For retrograde motion, equation (D41) is valid with use of $-\vec{i}$ in place of $\vec{i}$.

Velocity Components Relative to Moving Earth

From the values of $\vec{v_i}$, $\vec{v_j}$, and $\vec{v_k}$, and the velocity of Earth in its orbit v_E, components of the vector velocity $\vec{v_G}$ of the meteoric particle relative to the moving Earth were next determined. The vector velocity $\vec{v_G}$ always had approximately the same scalar magnitude as the velocity v_G given in reference 7. The components of $\vec{v_G}$ were determined with the equation

$$\vec{v_{ir}} = \left(\vec{v_i} \cdot \vec{i} - v_E\right)\vec{i} \tag{D42}$$

and with the two equations

$$\vec{v_{jr}} = \vec{v_j} \tag{D43}$$

$$\vec{v_{kr}} = \vec{v_k} \tag{D44}$$

TABLE V. - COMPUTED DATA FOR THREE SAMPLE METEORS

	Reference or equation number	Meteor number		
		6102	6430	8761
Page	ref. 7	35	39	34
Line	ref. 7	22	9	17
Direct or retrograde	----------	Direct	Direct	Retrograde
Orbital type	----------	Elliptical	Parabolic	Hyperbolic
γ, deg	----------	13	68	42
Cos Z_R	ref. 7	0.81	0.89	0.95
v_∞, km/sec	ref. 7	28.7	43.6	69.9
$F(Z_R)_{av}$	ref. 1	0.6272	0.4734	0.3863
φ_s	ref. 5	0.8581	0.6389	0.4713
a, AU	ref. 7	2.75	----------	5.87
q, AU	ref. 7	0.49	0.96	0.89
v_H, km/sec	ref. 7	38.5	42.4	44.2
$v_{e(s)}$ substituted for v_H, km/sec	----------	----------	42.14	----------
v_G, km/sec	ref. 7	26.7	42.1	68.9
b (AU)	eqs. (D5) or (D29)	1.567	----------	3.352
c (AU)	eqs. (D4), (D20), or (D28)	2.260	-0.960	6.761
e	eq. (D6)	0.822	----------	1.152
Cos θ	eqs. (D9), (D22), or (D31)	-0.1209	0.9200	0.7945
θ, deg	----------	96.94	23.07	37.39
dy/dx	eqs. (D12), (D26), or (D35)	-0.6995	-4.8990	-3.2046
φ, deg	eq. (D13)	55.03	11.54	17.33
λ, deg	eq. (D14)	41.92	11.54	20.06
$\lvert\vec{v}_j\rvert$, km/sec	eq. (D2)	25.72	8.427	15.163
$\lvert\vec{v}_i\rvert$, km/sec	eq. (D3)	28.65	41.30	41.51
$\lvert\vec{v}_k\rvert$, km/sec	eq. (D40)	6.443	38.28	27.78
$\vec{v}_i \cdot \vec{i}$, km/sec	eq. (D41)	27.92	15.47	-30.84
$\vec{v}_{ir} \cdot \vec{i}$, km/sec	eq. (D42)	-1.884	-14.33	-60.65
$\lvert\vec{v}_{jr}\rvert$, km/sec	eq. (D43)	25.72	8.428	15.163
$\lvert\vec{v}_{kr}\rvert$, km/sec	eq. (D44)	6.445	38.28	27.78
$\lvert\vec{v}_{ij}\rvert$, km/sec	eq. (E3)	25.79	16.626	62.52
$\lvert\vec{v}_{jk}\rvert$, km/sec	eq. (E4)	26.51	39.20	31.65
$\lvert\vec{v}_{ki}\rvert$, km/sec	eq. (E5)	6.714	40.88	66.71
φ_w	eq. (1)	1.997×10^{-6}	4.262×10^{-7}	7.931×10^{-8}
$\varphi_{cyl(i)}$	eq. (E6)	1.992×10^{-6}	4.003×10^{-7}	3.669×10^{-8}
$\varphi_{cyl(j)}$	eq. (E6)	5.044×10^{-7}	4.175×10^{-7}	7.734×10^{-8}
$\varphi_{cyl(k)}$	eq. (E6)	1.937×10^{-6}	1.698×10^{-7}	7.248×10^{-8}
$\varphi_{pl(i)}$	eq. (E2)	1.415×10^{-7}	1.464×10^{-7}	7.032×10^{-8}
$\varphi_{pl(j)}$	eq. (E2)	1.932×10^{-6}	8.607×10^{-8}	1.758×10^{-8}
$\varphi_{pl(k)}$	eq. (E2)	4.842×10^{-7}	3.910×10^{-7}	3.221×10^{-8}
$\varphi_{cyl(r)}$	eq. (F17)	1.568×10^{-6}	3.348×10^{-7}	6.229×10^{-8}
$\varphi_{pl(r)}$	eq. (F7)	9.984×10^{-7}	2.131×10^{-7}	3.966×10^{-8}
$\varphi_{cyl(i)0}$	eqs. (E10) and (E11)	1.417×10^{-9}	1.303×10^{-10}	1.832×10^{-11}
$\varphi_{cyl(i)1}$	eqs. (E10) and (E11)	4.258×10^{-9}	3.911×10^{-10}	5.501×10^{-11}
$\varphi_{cyl(i)24}$	eqs. (E10) and (E11)	1.831×10^{-7}	8.178×10^{-9}	1.419×10^{-9}
$\varphi_{cyl(i)25}$	eqs. (E10) and (E11)	2.731×10^{-7}	8.749×10^{-9}	1.579×10^{-9}
$\varphi_{cyl(i)26}$	eqs. (E10) and (E11)	3.904×10^{-7}	9.371×10^{-9}	1.778×10^{-9}
$\varphi_{cyl(i)79}$	eqs. (E10) and (E11)	0	0	0

APPENDIX E

USE OF ORTHOGONAL COMPONENTS OF METEOROID VELOCITIES RELATIVE TO EARTH TO OBTAIN DISTRIBUTIONS OF NORMAL COMPONENTS OF IMPACT VELOCITY

The two procedures outlined in the sections entitled Determination of Velocity Components Normal to Surfaces of Structures from Principal Components of Velocity Relative to Earth and Normal Velocity Distributions as Normalized Sums of Adjusted Unit Counts will be explained in detail here without a formal separation of the two procedures. The operation of the computer program in determining the distribution of normal impact velocity will be described on the basis of analogous hand tabulations, tables V and VI. As the procedure is simplest for impact upon planes, that case will be treated first.

Distribution of Normal Component of Impact Velocity Upon Planes

For planes an assumption was made that impacts would be statistically symmetrical relative to the two sides of the j and k planes. No such assumption was possible for the i plane. For the meteors treated, all impacts were on the same side of the j plane, and all on the same side of the k plane. Accordingly, velocity distributions could be determined for impacts on one side of each of these planes and could be assumed to apply to the other side also. A separate distribution was obtained for each side of the i plane. Negative values of $\vec{v_{ir}} \cdot \vec{i}$ indicated impact on the leading side of the i plane; positive values the reverse.

Table VI(a) is a skeleton tabulation for the j plane. It shows entries for three specific meteors and for several specific normal components of impact velocity. In table V appear identifications of the three sample meteors, the pertinent basic data as given in reference 7 or as calculated in the work of references 1 and 5, the results of various intermediate values calculated, and final values $\varphi_{pl(j)}$ entered in the tabulation of table VI(a). The entire procedure for arriving at the value $\varphi_{pl(j)}$ specifically for meteor 6102 will now be explained. (Table V also includes results for cylinders and spheres, which will be discussed later.)

The sources of the first 29 items in table V are obvious, have been clearly stated in the table, or have been explained in the main text or in preceding appendixes. Later items pertinent to the tabulation for the j plane in table VI(a) are $\vec{v_{ki}}$, φ_w from equation (1), and $\varphi_{pl(j)}$.

TABLE VI. - SKELETON TABULATION OF ADJUSTED UNIT COUNTS RELATIVE TO NORMAL COMPONENT OF IMPACT VELOCITY OF METEORS

[*Entries for most values of I and all entries for meteors other than 6102, 6430, and 8761 have been omitted.*]

(a) Plane whose normal points toward Sun

Meter serial number	Fully adjusted unit count for normal component of impact velocity between I and (I + 1), km/sec							Total of columns I = 0 to I = 79, $(\varphi_{pl(j)})$	Fully adjusted unit count for impact on randomly oriented plane, $(\varphi_{pl(r)})$
	I=0	I=7	I=8	I=9	I=15	I=25	I=79		
6102	0	0	0	0	0	1.932×10^{-6}	0	1.932×10^{-6}	9.984×10^{-7}
6430	0	0	8.607×10^{-8}	0	0	0	0	8.607×10^{-8}	2.131×10^{-7}
8761	0	0	0	0	1.758×10^{-8}	0	0	1.758×10^{-8}	3.966×10^{-8}
Totals	9.853×10^{-6}	3.831×10^{-4}	3.594×10^{-4}	3.283×10^{-4}	1.081×10^{-4}	4.402×10^{-5}	0	[a]4.583×10^{-3}	[a]3.786×10^{-3}
Percentage totals	.2150	8.360	7.842	7.164	2.233	.9606		100.00	----------

[a]Total impacts as percentage of statistically expected impacts on a randomly oriented plane surface = $(4.583\times10^{-3})/(3.786\times10^{-3}) \times 100 = 121.07$ percent.

(b) Cylinder whose axis points in direction of Earth movement

Meter serial number	Fully adjusted unit count for normal component of impact velocity between I and (I + 1), km/sec						Total of columns I=0 to I=79, $(\varphi_{cyl(i)})$	Fully adjusted unit count for impact on randomly oriented cylinder, $(\varphi_{cyl(r)})$
	I=0	I=1	I=24	I=25	I=26	I=79		
6102	1.417×10^{-9}	4.258×10^{-9}	1.831×10^{-7}	2.731×10^{-7}	3.904×10^{-7}	0	1.992×10^{-6}	1.568×10^{-6}
6430	1.303×10^{-10}	3.911×10^{-10}	8.178×10^{-9}	8.749×10^{-9}	9.371×10^{-9}	0	4.003×10^{-7}	3.348×10^{-7}
8761	1.832×10^{-11}	5.501×10^{-11}	1.419×10^{-9}	1.579×10^{-9}	1.778×10^{-9}	0	3.669×10^{-8}	6.229×10^{-8}
Totals	6.959×10^{-5}	2.076×10^{-4}	5.235×10^{-5}	3.451×10^{-5}	2.941×10^{-5}	0	[a]6.559×10^{-3}	[a]5.947×10^{-3}
Percentage totals	1.061	3.165	.7982	.5262	.4484	0	100.00	----------

[a]Total impacts as percentage of statistically expected impacts on a randomly oriented cylindrical surface = $(6.559\times10^{-3})/(5.947\times10^{-3}) \times 100 = 110.30$ percent.

The adjusted unit count φ_w must be modified for application to planes (and to cylinders, but not to spheres) to provide for the effect of variation of effective vulnerable area with the angle of incidence of the meteoroid. The modified adjusted unit count $\varphi_{pl(j)}$ is the result for the j plane. The modification is illustrated for the j oriented plane (and for later discussion of the j oriented cylinder) in figure 8.

In figure 8 the vector velocity of the meteoroid relative to the moving Earth is $\overrightarrow{v_G}$, which generally is not in the ecliptic plane. The projection of $\overrightarrow{v_G}$ upon the j plane is designated as $\overrightarrow{v_{ki}}$, and its projection on the axis normal to the j plane is $\overrightarrow{v_{jr}}$ (eq. (D43)). Now a unit of the j plane will project upon a plane oriented normally to $\overrightarrow{v_G}$ as an effective vulnerable area equal to the cosine of the angle i_{pl}, which is expressed as

$$i_{pl} = \tan^{-1} \frac{|\overrightarrow{v_{jr}}|}{|\overrightarrow{v_{ki}}|} \tag{E1}$$

As the weighting factor φ_w provides for the correct relative frequency of impact for angles of incidence always arbitrarily zero, the relative frequency of impact for other angles of incidence should be equal to the effective vulnerable area times φ_w. The modified adjusted unit count for the j plane should therefore be equal to the value of φ_w multiplied by the cosine of the angle i_{pl}, or

$$\left.\begin{aligned} \varphi_{pl(j)} &= \frac{|\overrightarrow{v_{jr}}|\,\varphi_w}{\left(|\overrightarrow{v_{jr}}|^2 + |\overrightarrow{v_{ki}}|^2\right)^{1/2}} \\ \varphi_{pl(i)} &= \frac{|\overrightarrow{v_{ir}}|\,\varphi_w}{\left(|\overrightarrow{v_{ir}}|^2 + |\overrightarrow{v_{jk}}|^2\right)^{1/2}} \\ \varphi_{pl(k)} &= \frac{|v_{kr}|\,\varphi_w}{\left(|\overrightarrow{v_{kr}}|^2 + |\overrightarrow{v_{ij}}|^2\right)^{1/2}} \end{aligned}\right\} \tag{E2}$$

In a similar manner,

The velocity components $\overrightarrow{v_{ij}}$, $\overrightarrow{v_{jk}}$, and $\overrightarrow{v_{ki}}$, scalar magnitudes for which are needed in equations (E2), are obviously obtainable with use of the values of $\overrightarrow{v_{ir}}$, $\overrightarrow{v_{jr}}$, and $\overrightarrow{v_{kr}}$ (eqs. (D42) to (D44)), as

$$\vec{v}_{ij} = \vec{v}_{ir} + \vec{v}_{jr} \tag{E3}$$

$$\vec{v}_{jk} = \vec{v}_{jr} + \vec{v}_{kr} \tag{E4}$$

$$\vec{v}_{ki} = \vec{v}_{kr} + \vec{v}_{ir} \tag{E5}$$

Now the modified adjusted unit count for the j plane $\varphi_{pl(j)}$ for meteor 6102 was 1.932×10^{-6} as shown in table V. The scalar magnitude of the normal component of impact velocity, $\vec{v}_{jr}$, was 25.72 km/sec. Hence, the modified adjusted unit count of 1.932×10^{-6} should properly be entered in table VI(a) in the column for I = 25. In a similar manner, the $\varphi_{pl(j)}$ values 8.607×10^{-8} and 1.758×10^{-8} for meteors 6430 and 8761 were entered in the proper columns for $|\vec{v}_{jr}|$ equal to 8.427 and for $|\vec{v}_{jr}|$ equal to 15.163, that is, in the columns for I = 8 and I = 15.

In the full tabulation, of which table VI(a) is only a skeleton, all meteors that were treated involved the same procedure, with entry of a value of $\varphi_{pl(j)}$ in the column having a value of I determined from the value $|\vec{v}_{jr}|$. In addition, an entry was made in the column for "Total of columns I = 0 to I = 79." This entry was always the same as $\varphi_{pl(j)}$. As will be seen later, the procedure was somewhat different for cylinders and spheres. (The last column of table VI(a) and the footnote may be ignored until values of φ_g are discussed in appendix F.)

After all meteors meeting the necessary conditions had been so treated, the columns for I = 0 to 79 were totaled, and the results were converted to percentages as shown in the last line of the table. The percentage results were entered in the appropriate column of table IV and were plotted as the circular symbols in figure 1(c).

The i and k oriented planes were treated in the same manner, in tabulations similar to that represented by table VI(a), with use of values of $\varphi_{pl(i)}$ and $\varphi_{pl(k)}$ and values of $\vec{v}_{ir} \cdot \vec{i}$ and $|\vec{v}_{kr}|$ from table V. For the i oriented plane, however, a separate tabulation was made for each side. Negative values of $\vec{v}_{ir} \cdot \vec{i}$ called for entry of $\varphi_{pl(i)}$ in the appropriate column of the tabulation for the leading side of the plane, positive values the opposite. The resulting velocity distributions for the two sides of the i plane and for the k plane appear in table IV and are plotted as the circular symbols in figure 1(a), (b), and (d).

As has been explained, only meteors reaching Earth from the side of the j plane opposite the Sun and from the north side of the k plane have been considered. However, any meteoroid arriving from other directions symmetrically relative to either or both of those planes would strike the i, j, or k plane with the same normal component of relative velocity. Hence, with the assumption of symmetry of meteoroid influx relative to the j and k planes, the method of determining distribution of normal components of

impact velocity that has been described, when applied to the one quadrant of space that is totally covered, should be valid for impact from all directions. This same statement will apply to the method used for cylinders.

Distribution of Normal Component of Impact Velocity Upon Cylinders

The manner of determination of distributions of normal components of impact velocity upon cylinders was similar to that for planes. However, the i, j, and k oriented cylinders could all be treated in the same manner, without the need for distinction between two sides of any of them. The desired result, for each orientation of a cylinder, applies to all parts of the surface collectively.

A skeleton tabulation for an i oriented cylinder appears in table VI(b). It is just like table VI(a) and is made up from data given in table V in a manner that will now be described.

In table V the items to and including φ_w have been explained. The items following φ_w that are pertinent to the distribution of normal component of impact velocity upon the i cylinder are $\varphi_{cyl(i)}$, and $\varphi_{cyl(i)n}$ with n equal to 0, 1, 24, 25, 26, and 79.

The modified adjusted unit count $\varphi_{cyl(i)}$ serves the same purpose for the i cylinder as $\varphi_{pl(j)}$ serves for the j plane. This analogous modification of the adjusted unit count for the i oriented cylinder may be referred to the worst case, in which $\overrightarrow{v_G}$ would lie within the i plane. With reference to such a case, as may be seen in figure 8, the effective vulnerable area presented by the cylinder would vary as the cosine of the angle i_{cyl}, or as the sine of i_{pl} given for the case of the j plane by equation (E1). Hence,

$$\left.\begin{aligned}
\varphi_{cyl(i)} &= \frac{|\overrightarrow{v_{jk}}|\,\varphi_w}{\left(|\overrightarrow{v_{ir}}|^2 + |\overrightarrow{v_{jk}}|^2\right)^{1/2}} \\
\varphi_{cyl(j)} &= \frac{|\overrightarrow{v_{ki}}|\,\varphi_w}{\left(|\overrightarrow{v_{jr}}|^2 + |\overrightarrow{v_{ki}}|^2\right)^{1/2}} \\
\varphi_{cyl(k)} &= \frac{|\overrightarrow{v_{ij}}|\,\varphi_w}{\left(|\overrightarrow{v_{kr}}|^2 + |\overrightarrow{v_{ij}}|^2\right)^{1/2}}
\end{aligned}\right\} \qquad \text{(E6)}$$

For a cylinder the modified adjusted unit count such as $\varphi_{cyl(i)}$ had to be distributed to the various columns for $I = 0$ to $I = n$, where n is the highest integral value less than the maximum normal component of impact velocity possible. Such procedure was necessary because oblique impacts would allow any normal velocity component from zero to the full value of $|\overrightarrow{v_{ij}}|$, $|\overrightarrow{v_{jk}}|$, or $|\overrightarrow{v_{ki}}|$, as the case might be. That the values $|\overrightarrow{v_{ij}}|$, $|\overrightarrow{v_{jk}}|$, and $|\overrightarrow{v_{ki}}|$ are the maximum possible normal components may be easily seen. For example, the surface of an i oriented cylinder would encounter normal impact velocities dependent only on the vector velocity $\overrightarrow{v_{jk}}$. The only component of $\overrightarrow{v_G}$ missing from $\overrightarrow{v_{jk}}$ is parallel to the axis of the cylinder and hence can contribute nothing toward normal impact velocity on the surface. Hence, the maximum normal component of velocity on the surface would have the scalar magnitude $|\overrightarrow{v_{jk}}|$, the minimum would be zero.

Sketch (d) illustrates the manner of partition of $\varphi_{cyl(i)}$. The i plane is shown, as

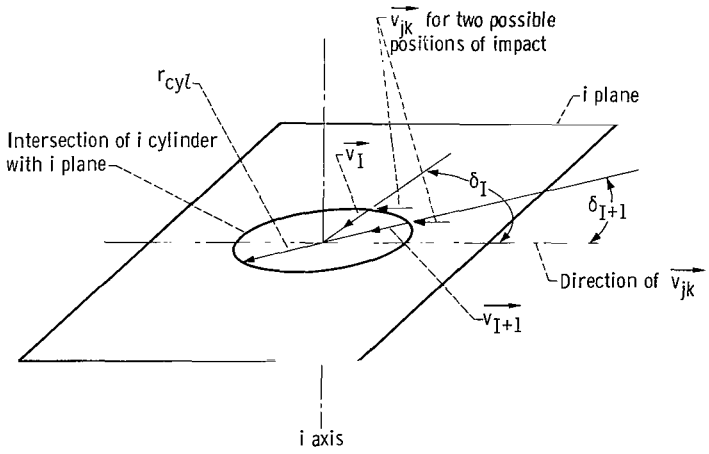

(d)

well as its circular intersection with an i oriented cylinder of radius r_{cyl}. The angles at which the normal component of impact velocity on the cylindrical surface will be equal to I and I + 1 are assumed as δ_I and δ_{I+1}.

Now the normal impact velocity with impact at the angular position δ_I will be

$$|\overrightarrow{v_i}| = |\overrightarrow{v_{jk}}| \cos \delta_I \tag{E7}$$

or, with $|\overrightarrow{v_I}|$ equal to I,

$$\delta_I = \cos^{-1}\left(\frac{I}{|\overrightarrow{v_{jk}}|}\right) \tag{E8}$$

Of many hypothetical impacts of meteoroids, each with a given velocity component $\overrightarrow{v_{jk}}$, the fraction that will have a component of velocity normal to the cylindrical surface within the range from I to I + 1 must be equal to the distance between the two vectors $\overrightarrow{v_{jk}}$ as shown in the sketch divided by the distance r_{cyl}. Hence, such fraction is

$$\varphi_I = \frac{r_{cyl}(\sin \delta_I - \sin \delta_{I+1})}{r_{cyl}} \tag{E9}$$

From equations (E8) and (E9),

$$\varphi_I = \sqrt{1 - \left(\frac{I}{|\overrightarrow{v_{jk}}|}\right)^2} - \sqrt{1 - \left(\frac{I+1}{|\overrightarrow{v_{jk}}|}\right)^2} \tag{E10}$$

and the part of the modified adjusted unit count $\varphi_{cyl(i)}$ that must be entered in the I column of table VI(b) is

$$\varphi_{cyl(i)I} = \varphi_{cyl(i)}\,\varphi_I \tag{E11}$$

For any case in which I + 1 is greater than and I is smaller than $|\overrightarrow{v_{jk}}|$, zero must be substituted for the second term in the right-hand side of equation (E10). When I is equal to or greater than $|\overrightarrow{v_{jk}}|$, $\varphi_{cyl(i)I}$ must be arbitrarily zero without reference to equations (E10) and (E11).

For the three sample meteors, the values of $\varphi_{cyl(i)}$, $\varphi_{cyl(j)}$, and $\varphi_{cyl(k)}$ found with use of equations (E6) are shown in table V. Also shown, for each meteor, are the values of $\varphi_{cyl(i)n}$ for n = 0, 1, 24, 25, 26, and 79. Those values of $\varphi_{cyl(i)n}$ were entered in the proper positions in the skeleton tabulation shown in table VI(b).

After such entries in the full tabulation were completed for all meteors treated, the procedure was exactly as with planes. For j and k orientations of cylinders, similar tabulations were made with use of equations analogous to (E10) and (E11). The results are tabulated in table IV and plotted as the circular points in the three parts of figure 2.

Distribution of Normal Component of Impact Velocity Upon Spheres

A tabulation not shown even in skeleton form but similar to those of table VI was provided for all impacts, normal or oblique, on the surface of a sphere. The results were as shown in the last column of table IV and as shown by the plotted circular points in figure 3. (The second column of table IV is a recapitulation of results explained and discussed in ref. 4.)

As a sphere presents the same size and shape of surface with the same relative orientation for a meteoroid flux from any direction, no directional characteristics of the relative velocity v_G need be considered. Any meteor can impact a sphere with normal component of the impact velocity within the range from zero to the full value of v_G. No consideration needs to be given to a modification of φ_w for variation in effective vulnerable area similar to those that produced the modified adjusted unit counts $\varphi_{pl(j)}$ or $\varphi_{cyl(j)}$. That is, φ_w is usable directly instead of $\varphi_{pl(j)}$ or $\varphi_{cyl(j)}$.

The value of the adjusted unit count φ_w, however, does need to be distributed among the various values of I from $I = 0$ to $I = n$, where n is the largest integer that is less than v_G. Sketch (e) illustrates the principle of such distribution. In that sketch, a hemisphere is shown above an intersecting plane. Such plane may be arbitrarily selected, but containing an axis that passes through the center of the sphere in a direction parallel to $\vec{v_G}$. Also shown, at the right, is a plane normal to the direction of $\vec{v_G}$. Projection lines extending from the hemisphere to the plane at the right represent three concentric cylindrical surfaces: (1) circumscribing the hemisphere, that is, with all elements of

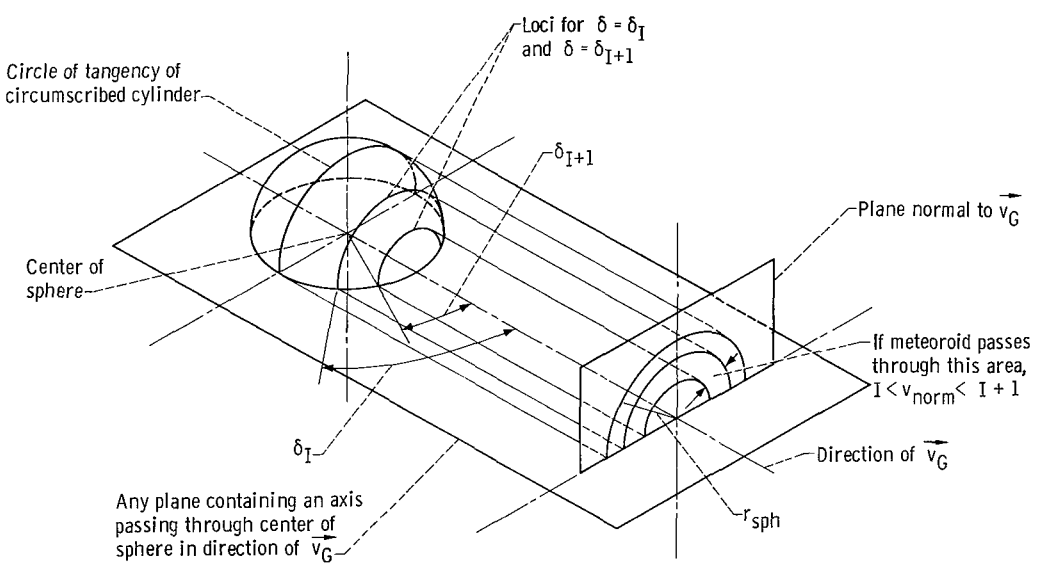

(e)

the cylindrical surface tangent to the hemisphere, (2) with all cylindrical elements passing through the circular locus on the hemisphere for values of the angle δ equal to δ_I, and (3) the same as (2) but for δ_{I+1}. With angles δ_I and δ_{I+1} having the same significance as earlier, equations (E7) and (E8) apply with substitution of v_G for $|\overrightarrow{v_{ki}}|$. But, here, the probability that the normal impact velocity upon the sphere will be between I and I + 1 must be equal to the ratio of two areas within the plane at the right of the sketch. That ratio must be the area between the concentric cylinders that were enumerated (2) and (3), divided by the total area within the cylinder enumerated (1). Hence, equation (E9) is replaced with

$$\varphi_I = \frac{r_{sph}^2\left(\sin^2 \delta_I - \sin^2 \delta_{I+1}\right)}{r_{sph}^2} \tag{E12}$$

in which r_{sph} is radius of the sphere. Equation (E10), then is replaced by

$$\varphi_I = \left(\frac{I+1}{v_G}\right)^2 - \left(\frac{I}{v_G}\right)^2 = \frac{2I+1}{v_G^2} \tag{E13}$$

and equation (E11) is replaced by the following expression for the fractional adjusted unit count for normal velocity components on a spherical surface,

$$\varphi_{sph(I)} = \varphi_w \varphi_I \tag{E14}$$

APPENDIX F

CALCULATION OF CONCENTRATION FACTORS FOR METEOROID IMPACT UPON VARIOUSLY ORIENTED STRUCTURES

For use in calculation of necessary armor thickness a concentration factor, or ratio, φ_g is needed by which the expected frequency of impact of meteoroids upon one side of a randomly oriented surface may be multiplied to yield the frequency of impact upon a given structure with a given orientation. For a sphere, the ratio φ_g is always unity because in effect the sphere is a randomly oriented surface, having differential surface areas facing impartially in all possible directions. But, for planes and cylinders with i, j, and k orientations, the value of φ_g is never unity.

For one example each of a plane and a cylinder the total of the next-to-last column in table V(a) or (b) provides an important portion of the desired ratio φ_g, which will be designated φ'_g. The significance of the factors $\varphi_{m(n)}$ (m signifies pl or cyl, and n signifies i, j, or k), as they appear in table V is explained in appendix E. The value of the factor φ'_g as defined is the total of those values of $\varphi_{m(n)}$ for the pertinent significance of m and n. From the explanation in appendix E, therefore, the value of φ'_g is the total of a modified adjusted unit count for all meteors treated, for the given orientation of the structure, expressed as

$$\varphi'_g = \sum \varphi_{m(n)} = \sum \varphi_{or}\varphi_w \tag{F1}$$

where the summation is performed for all meteors treated and where φ_{or} is a factor relating the probability of impact by the particular meteoroid under consideration upon the structure as oriented, relative to the probability of impact by that same meteoroid upon the same structure with an arbitrary basic orientation relative to the direction of motion of the meteoroid. For planes, that basic orientation was normal to the path of each meteoroid. For cylinders the basic orientation was with the cylinder axis parallel to any arbitrarily chosen line perpendicular to the meteoroid path.

Now, from equation (F1), an average value of frequency of impact upon the structure as oriented, as a fraction or multiple of the frequency of impact with the basic orientation relative to movement of each meteoroid, will be

$$\varphi_{or(av)} = \frac{\varphi'_g}{\sum \varphi_w} \tag{F2}$$

The manner of obtaining a value of φ_g from the value of $\varphi_{or(av)}$, for planes and cylinders, will now be described.

Concentration Factor for Planes

For a plane $\sum \varphi_w$ as used in equation (F2) will be regarded as the statistical frequency of impact per unit area on one arbitrarily chosen side of that area by all sporadic meteors from the single quadrant of space treated, in unspecified units, under the assumption that the chosen side of that area is always oriented to face each oncoming meteoroid normally. (With different units, $\sum \varphi_w$ could as well be regarded as the frequency of impact upon one arbitrarily chosen side of a randomly oriented surface.)

Now the one side of a unit area arbitrarily oriented to face any oncoming meteoroid normally will receive the same frequency of impacts as the external surface of a sphere of one unit cross section (radius $\pi^{-1/2}$). But the external surface of that sphere, in effect randomly oriented, will amount to four units of area. Hence, the frequency of impact upon it per unit area of outer surface will be one-quarter as great as for the chosen side of the always normally oriented unit area. So

$$\sum \varphi_{w(r)} = \frac{1}{4} \sum \varphi_w \tag{F3}$$

where $\varphi_{w(r)}$ is the frequency of impacts upon one side of a randomly oriented surface by meteoroids from the single quadrant of space that was treated. By the same reasoning,

$$\varphi_{w(r)} = \frac{1}{4} \varphi_w \tag{F4}$$

where $\varphi_{w(r)}$ is the same adjusted unit count as φ_w, but referred to one side of a randomly oriented area, instead of the always normal orientation.

Now conversion of equation (F2) to an expression for frequency of impact relative to one side of a randomly oriented surface (for the one quadrant only) is analogous to a change of units. That is, equation (F2) will give the same result, but related to the random orientation rather than the normal orientation, if $\varphi_{w(r)}$ of equation (F4) is substituted for φ_w in the denominator of the right-hand side to give

$$\varphi_{g(qu)} = \frac{\varphi'_g}{\sum \varphi_{w(r)}} \tag{F5}$$

Now $\varphi_{g(qu)}$ of equation (F5) would be the desired end result φ_g except that only impacts from one quadrant of space have been considered. For one side only of the j or k oriented plane, adding the symmetrical flux from three additional quadrants of space would only double the frequency of impact, because meteoroids from two of those quadrants would impact the other side of each plane. But the impacts on a randomly oriented surface would be multiplied by four. Hence, for the j or k plane,

$$\varphi_g = \frac{1}{2}\,\varphi_{g(qu)} = \frac{\varphi'_g}{2\sum \varphi_{w(r)}} = \frac{\varphi'_g}{\frac{1}{2}\sum \varphi_w} \tag{F6}$$

and, with the following definition,

$$\varphi_{pl(r)} = \frac{1}{2}\,\varphi_w \tag{F7}$$

equation (F6) becomes

$$\varphi_g = \frac{\varphi'_g}{\sum \varphi_{pl(r)}} \tag{F8}$$

For either side of an i oriented plane, addition of symmetrical impacts from the four quadrants of space not treated would multiply the impacts by four, just as with the randomly oriented surface. Hence, for either side of the i plane, equation (F6) is replaced by

$$\varphi_g = \varphi_{g(qu)} = \frac{\varphi'_g}{\sum \varphi_{w(r)}} = \frac{\varphi'_g}{\frac{1}{4}\sum \varphi_w} \tag{F9}$$

and equation (F7) becomes

$$\varphi_{pl(r)} = \frac{1}{4}\,\varphi_w \tag{F10}$$

for use in equation (F8).

For the j plane as an example, values of $\varphi_{pl(r)}$ from equation (F7), as shown in

table V, were entered in the last column of table VI(a). Hence, the total of that column, 3.786×10^{-3}, is the value of $\sum\varphi_{pl(r)}$ needed for use in equation (F8). Accordingly, as shown in the footnote of the table, equation (F8) yielded a value of 121.07 percent for φ_g.

The procedure for the k plane was the same. For each side of the i plane the procedure was similar, but with use of equation (F10) instead of (F7). Also, the summation $\sum\varphi_{pl(r)}$ was made for all meteoroids treated, not just those that impacted the pertinent side of the i plane.

Concentration Factor for Cylinders

The procedure for an i, j, or k cylinder was like that for the j and k planes except that a different expression was required than equation (F7). For the i oriented cylinder, as an example, the value of φ'_g for use in equation (F2) was the total of the next-to-last column in table VI(b).

With the basic orientation of a cylinder of length λ_{cyl} and radius r_{cyl}, the total cylindrical surface area would be

$$S_{cyl} = 2\pi r_{cyl}\lambda_{cyl} \tag{F11}$$

and the equivalent area presented normally to a meteoroid path would be

$$A_{eff} = 2r_{cyl}\lambda_{cyl} \tag{F12}$$

The same equivalent area would be offered by a sphere of radius

$$r_{sph} = \sqrt{\frac{2r_{cyl}\lambda_{cyl}}{\pi}} \tag{F13}$$

The external surface of such sphere would have an area

$$S_{sph} = 4\pi r_{sph}^2 = 8r_{cyl}\lambda_{cyl} \tag{F14}$$

From equations (F11) and (F14),

$$\frac{S_{sph}}{S_{cyl}} = \frac{4}{\pi} \tag{F15}$$

But the surfaces S_{sph} and S_{cyl} should receive the same number of impacts, and the surface S_{sph} is in effect randomly oriented. Hence, the impacts per unit area upon the surface S_{sph} should exceed those upon S_{cyl} by the ratio $\pi/4$. Accordingly, the equivalent of equation (F4) for use with the cylinders should be

$$\varphi_{w(r)} = \frac{\pi}{4} \varphi_w \tag{F16}$$

Addition of impacts by meteoroids from three additional quadrants, for i, j, or k cylinders, would multiply total impacts by four, just as with a randomly oriented surface. Hence, by the same reasoning as with planes, equations (F7) and (F8) become

$$\varphi_{cyl(r)} = \frac{\pi}{4} \varphi_w \tag{F17}$$

and

$$\varphi_g = \frac{\varphi'_g}{\sum \varphi_{cyl(r)}} \tag{F18}$$

The method of application of equations (F17) and (F18) in the example shown in tables V and VI(b) is identical to the example for a plane previously discussed.

REFERENCES

1. Miller, C. D.: Simultaneous Correction of Velocity and Mass Bias in Photography of Meteors. NASA TR R-280, 1968.

2. Miller, C. D.: Unaccelerated Geocentric Velocities and Influx Rates of Sporadic Photographic Meteors. NASA TN D-5245, 1969.

3. Miller, C. D.: Empirical Analysis of Unaccelerated Velocity and Mass Distributions of Photographic Meteors. NASA TN D-5710, 1970.

4. Miller, C. D.: Necessary Thickness of Randomly Oriented Armor for Meteoroid Protection. NASA TN D-5763, 1970.

5. Albers, Lynn U.; and Diedrich, George: Computation of Spatial Bias Correction Factors for a Collection of Meteors. NASA TN D-5711.

6. Hawkins, Gerald S.; and Upton, Edward K. L.: The Influx Rate of Meteors in the Earth's Atmosphere. Astrophys. J., vol. 128, no. 3, Nov. 1958, pp. 727-735.

7. McCrosky, Richard E.; and Posen, Annette: Orbital Elements of Photographic Meteors. Smithsonian Contributions to Astrophysics, vol. 4, no. 2, 1961, pp. 15-84.

8. Verniani, F.: On the Density of Meteoroids. II. The Density of Faint Photographic Meteors. 'Il Nuovo Cimento, vol. 33, no. 4, Aug. 16, 1964, pp. 1173-1184.

9. Hawkins, Gerald S.: Radar Determination of Meteor Orbits. Astronomical J., vol. 67, no. 5, June 1962, pp. 241-244.

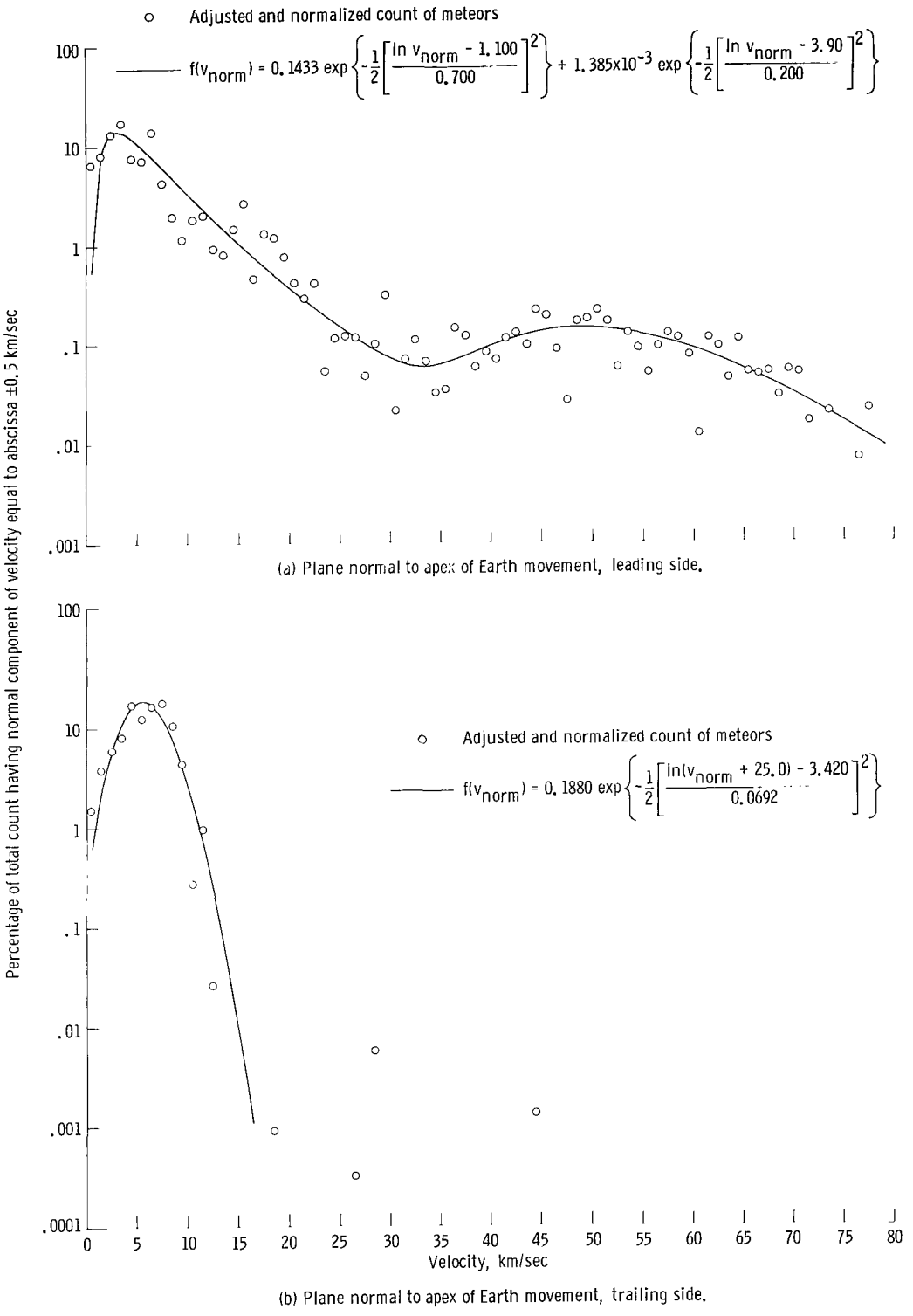

Figure 1. - Distribution of normal component of impact velocity of meteoroids upon a plane surface with three principal orientations.

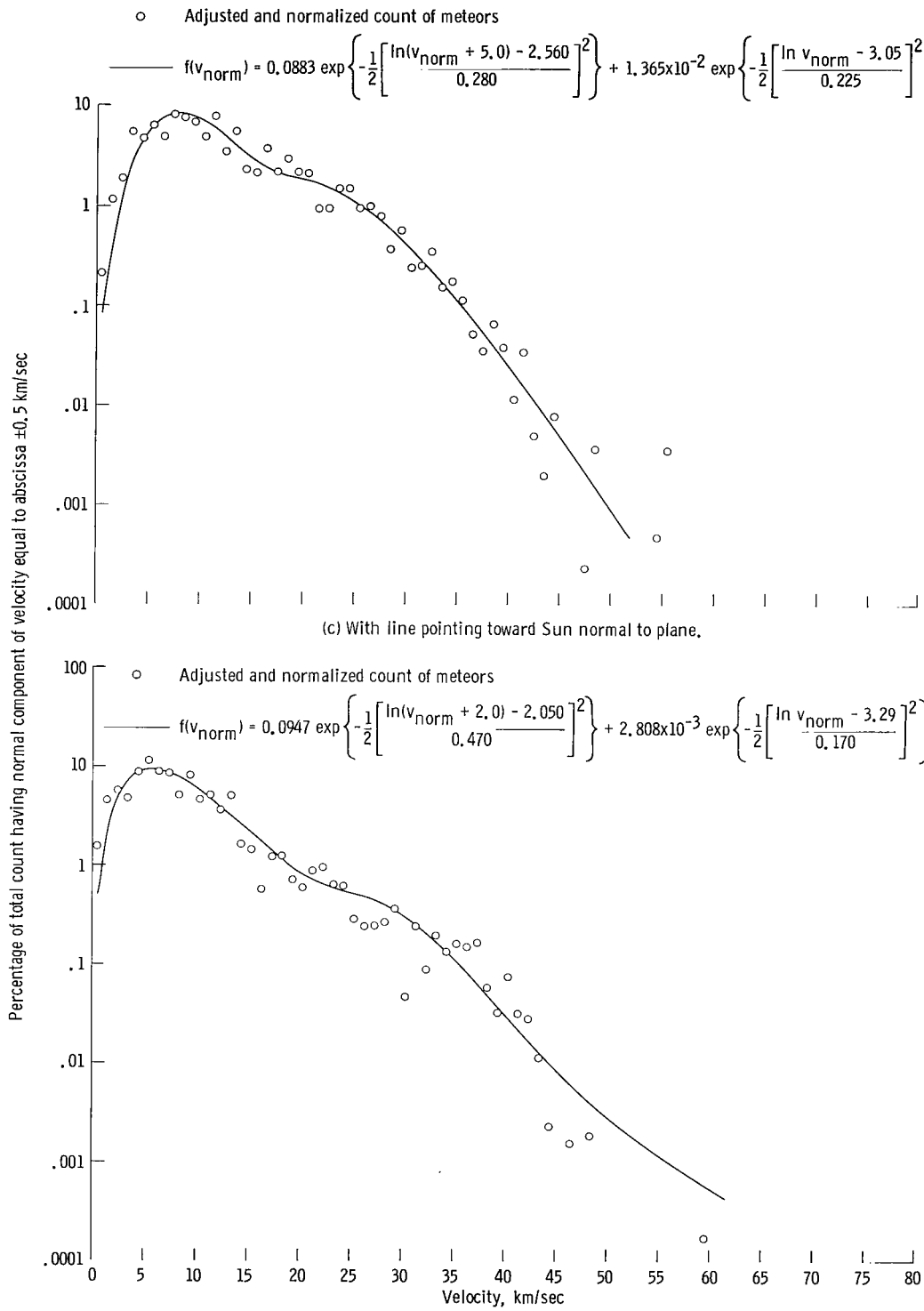

Figure 1. - Concluded.

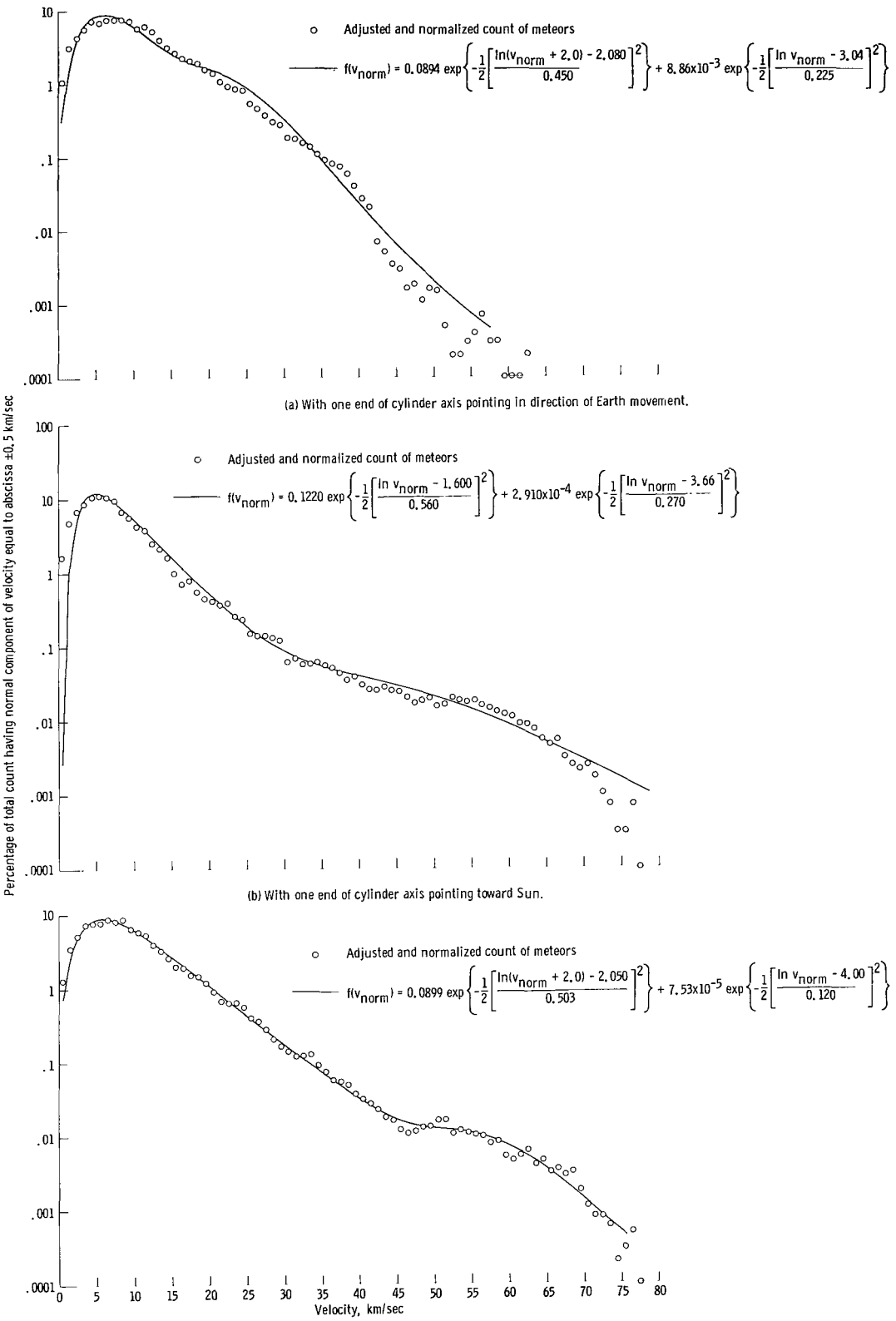

Figure 2. - Distribution of normal component of impact velocity of meteoroids upon cylindrical surface with three principal orientations.

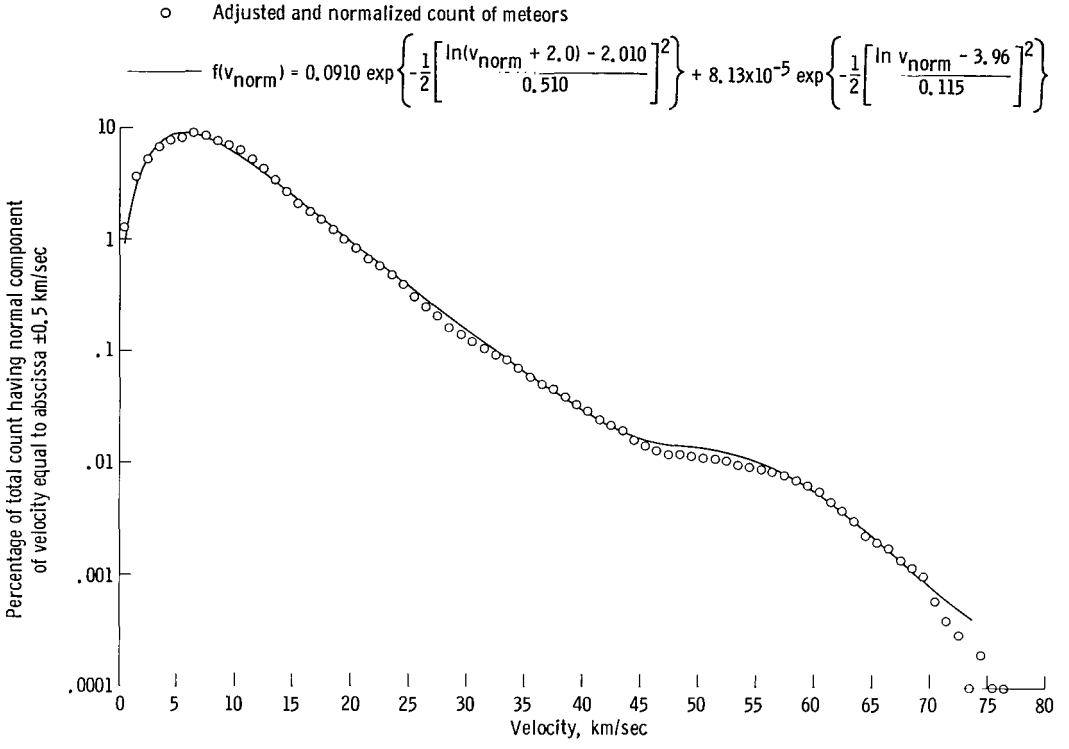

Figure 3. - Distribution of normal component of impact velocity of meteoroids upon surface of a sphere.

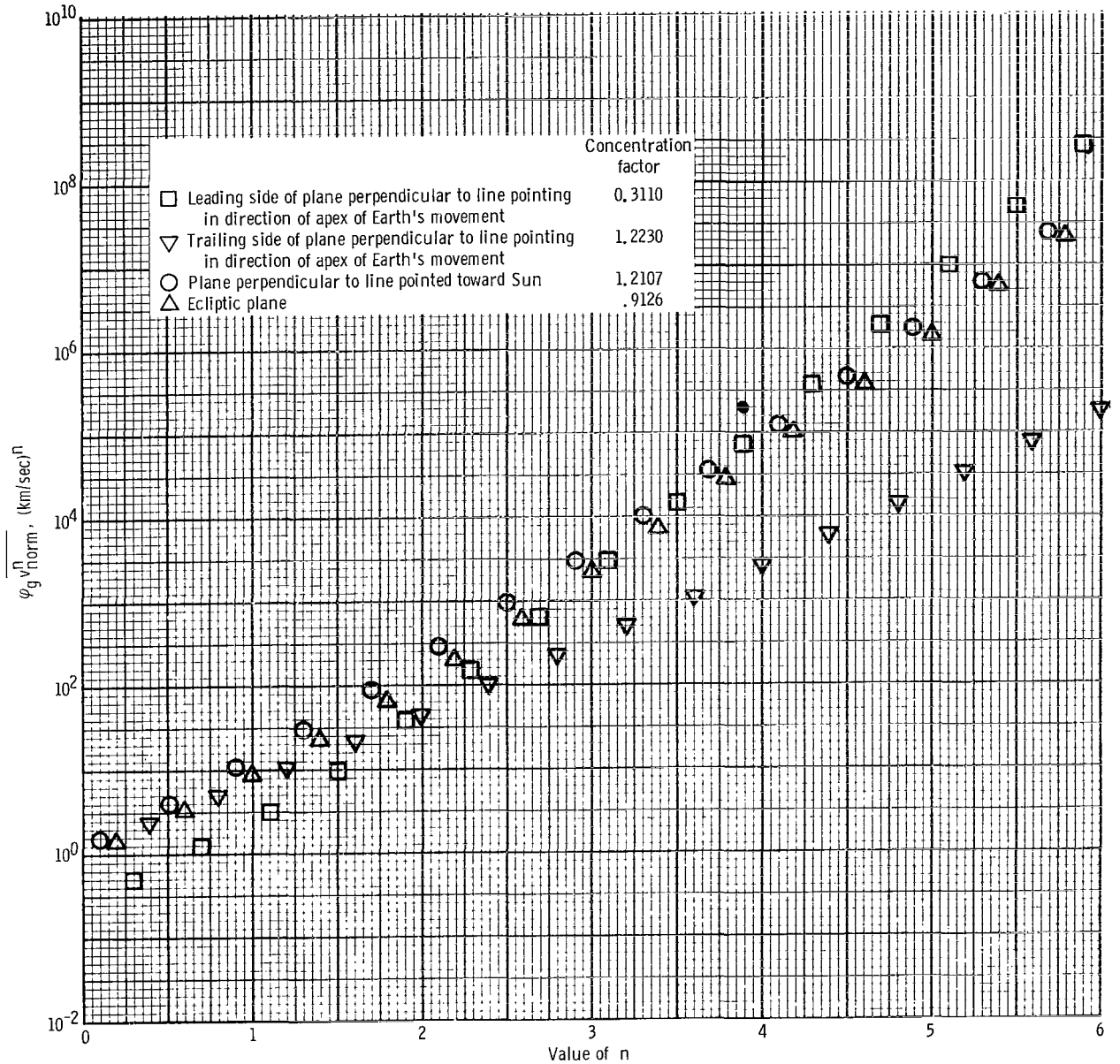

Figure 4. - Product of concentration factor and average n^{th} power of normal component of impact velocity of meteoroids on surface of a plane.

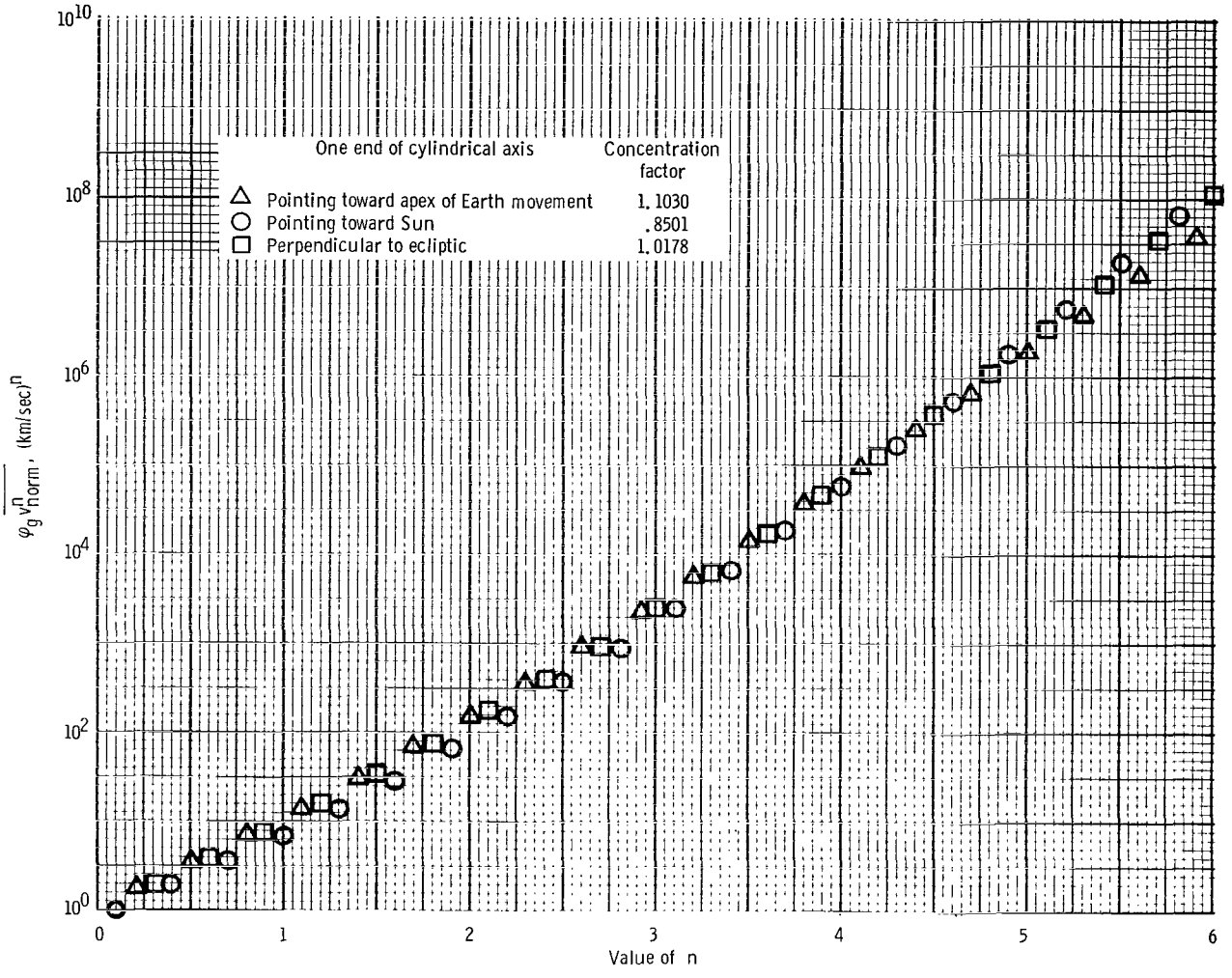

Figure 5. - Product of concentration factor and average n^{th} power of normal component of impact velocity of meteoroids on cylindrical surface.

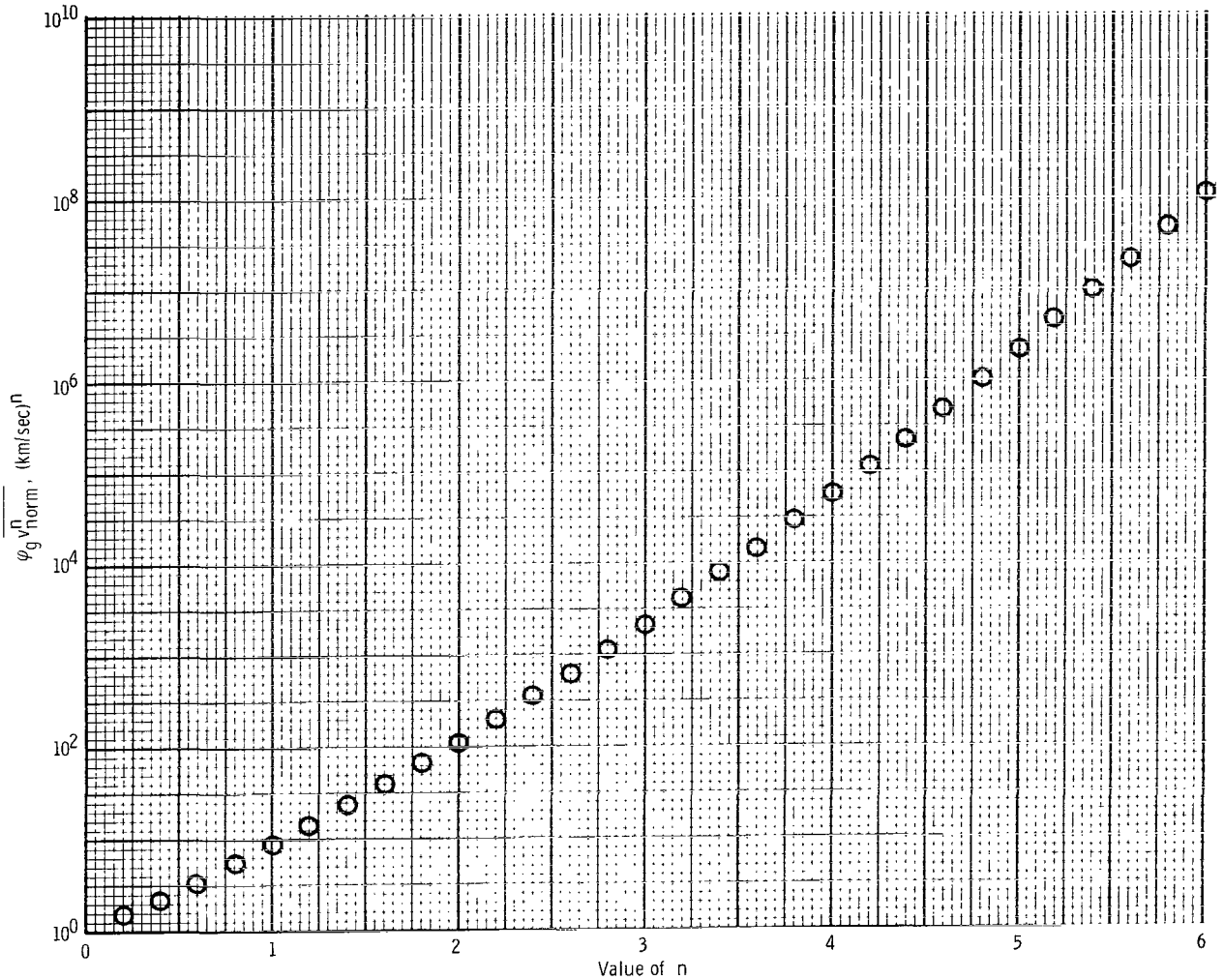

Figure 6. - Average n^{th} power of normal component of impact velocity of meteoroids on surface of a sphere.

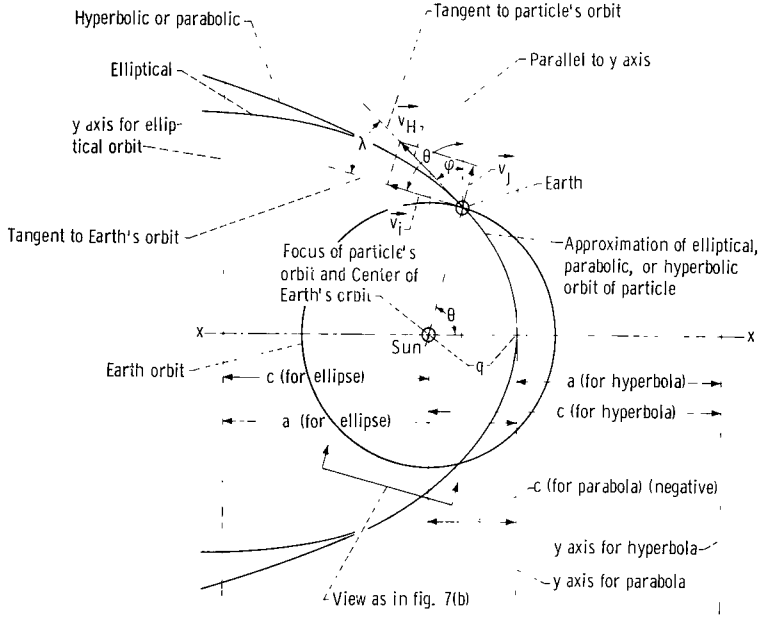

(a) Orbit of particle treated as within ecliptic plane.

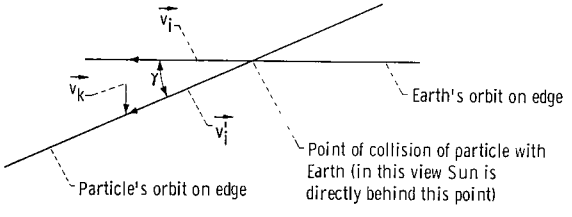

(b) View from position shown in part (a).

Figure 7. - View of orbits of particle and Earth.

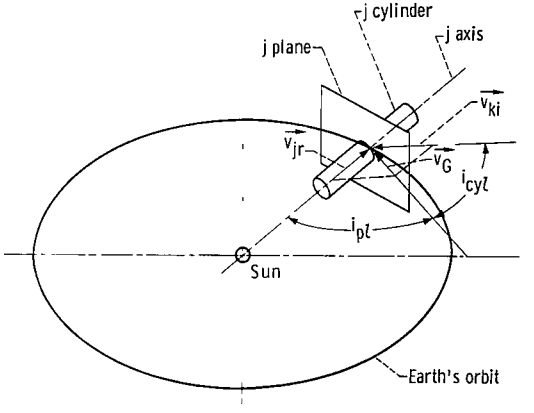

Figure 8. - Effect of incidence angle of meteoroid impact on vulnerable area of plane or cylinder.

04U 001 55 51 3DS 70272 00903
AIR FORCE WEAPONS LABORATORY /WLOL/
KIRTLAND AFB, NEW MEXICO 87117

ATT E. LOU BOWMAN, CHIEF,TECH. LIBRARY

"The aeronautical and space activities of the United States shall be conducted so as to contribute . . . to the expansion of human knowledge of phenomena in the atmosphere and space. The Administration shall provide for the widest practicable and appropriate dissemination of information concerning its activities and the results thereof."

—NATIONAL AERONAUTICS AND SPACE ACT OF 1958

NASA SCIENTIFIC AND TECHNICAL PUBLICATIONS

TECHNICAL REPORTS: Scientific and technical information considered important, complete, and a lasting contribution to existing knowledge.

TECHNICAL NOTES: Information less broad in scope but nevertheless of importance as a contribution to existing knowledge.

TECHNICAL MEMORANDUMS: Information receiving limited distribution because of preliminary data, security classification, or other reasons.

CONTRACTOR REPORTS: Scientific and technical information generated under a NASA contract or grant and considered an important contribution to existing knowledge.

TECHNICAL TRANSLATIONS: Information published in a foreign language considered to merit NASA distribution in English.

SPECIAL PUBLICATIONS: Information derived from or of value to NASA activities. Publications include conference proceedings, monographs, data compilations, handbooks, sourcebooks, and special bibliographies.

TECHNOLOGY UTILIZATION PUBLICATIONS: Information on technology used by NASA that may be of particular interest in commercial and other non-aerospace applications. Publications include Tech Briefs, Technology Utilization Reports and Notes, and Technology Surveys.

Details on the availability of these publications may be obtained from:

SCIENTIFIC AND TECHNICAL INFORMATION DIVISION

NATIONAL AERONAUTICS AND SPACE ADMINISTRATION

Washington, D.C. 20546